CarelessWhisper: Turning Whisper into a Causal Streaming Model

Tomer Krichli ⦿, Bhiksha Raj ⦿, *IEEE Fellow*, Joseph Keshet ⦿, *Senior Member, IEEE*

Abstract—**Automatic Speech Recognition (ASR) has seen remarkable progress, with models like OpenAI Whisper and NVIDIA Canary achieving state-of-the-art (SOTA) performance in offline transcription. However, these models are not designed for streaming (online or real-time) transcription, due to limitations in their architecture and training methodology. We propose a method to turn the transformer encoder-decoder model into a low-latency streaming model that is careless about future context. We present an analysis explaining why it is not straightforward to convert an encoder-decoder transformer to a low-latency streaming model. Our proposed method modifies the existing (non-causal) encoder to a causal encoder by fine-tuning both the encoder and decoder using Low-Rank Adaptation (LoRA) and a weakly aligned dataset. We then propose an updated inference mechanism that utilizes the fine-tune causal encoder and decoder to yield greedy and beam-search decoding, and is shown to be locally optimal. Experiments on low-latency chunk sizes (less than 300 msec) show that our fine-tuned model outperforms existing non-fine-tuned streaming approaches in most cases, while using a lower complexity. Additionally, we observe that our training process yields better alignment, enabling a simple method for extracting word-level timestamps. We release our training and inference code, along with the fine-tuned models, to support further research and development in streaming ASR.**

Index Terms—**Automatic Speech Recognition, Streaming ASR, Whisper, Causal Masking, Low Latency**

I. INTRODUCTION

AUTOMATIC speech recognition (ASR) systems have made remarkable progress in recent years, driven in large part by the development of powerful neural architectures. Since the introduction of the Transformer architecture [39], a wide range of strategies have been proposed to adapt it to ASR tasks. These include models based solely on the Transformer encoder [1], [12], [33], others employ Transformer decoder-only architectures [2], [37], and some adopt the full Transformer encoder-decoder model [25], [29]. The most well-known model in the latter category is Whisper [29], trained on 680,000 hours of weakly supervised speech data across 100 languages. Its broad linguistic coverage and robustness to noise have established it as a strong baseline for multilingual ASR.

In offline settings, Whisper offers near-unmatched performance in terms of noise robustness and multilingual versatility. However, its non-causal encoder limits its ability to process streaming input. Several works [23], [41] explore using Whisper without additional training, employing heuristic methods to enable streaming. *Simul-Whisper* [41], for example, uses

alignment heads to decide when to emit a token, while *Ufal-Whisper* [23] relies on an audio buffer and a local agreement algorithm [20] to generate real-time transcriptions. While both avoid fine-tuning, their inference pipelines require padding the input to 30 seconds at every step, resulting in sub-optimal computational efficiency.

U2-Whisper [46] proposes fine-tuning Whisper encoder using a causal mask and trains a new connectionist temporal classification (CTC) [8] head from scratch. During inference, it performs two-pass decoding—first predicting tokens using the CTC head, then ranking candidates with Whisper decoder. WhisperFlow [42] proposed to fine-tune Whisper encoder to detect a fixed hush word, that is appended at the end of each chunk, adapting Whisper to a streaming case.

We propose a method to transform the Whisper encoder-decoder architecture into a fully streaming model with low latency and without dependence on future context. Unlike prior approaches that either avoid training or require auxiliary heads and multi-pass decoding, our method directly adapts Whisper's core components for causal, efficient inference. Specifically, we modify the original non-causal encoder to operate causally and fine-tune both the encoder and decoder using Low-Rank Adaptation (LoRA) [13] on a weakly aligned dataset. We inject LoRA layers into both encoder and decoder attention modules to adapt the model to streaming representations. Training is performed using a cross-entropy loss on weakly aligned datasets, aligned using forced alignment [24]. This approach removes the need for CTC loss or architectural changes. We also introduce a novel streaming training strategy that circumvents the need to iterate over all possible audio sub-segments. This lightweight adaptation enables the model to function in streaming scenarios. To support efficient real-time inference, we introduce a decoding strategy that leverages the fine-tuned causal components to perform both greedy and beam search decoding. Our analysis demonstrates that the resulting outputs are locally optimal, providing a compelling balance between accuracy and latency in streaming ASR applications.

The paper is organized as follows. Section II surveys prior work, Section III outlines the problem setup, Section IV details our training and inference methods, Section V provides efficiency analysis, Section VI details the training process, Section VII presents experimental setup, displays and discusses results, and Section VIII concludes with future directions.

For implementation details, refer to our GitHub repository[1] and the Hugging Face demo page[2].

---

[1]https://github.com/tomer9080/CarelessWhisper-streaming
[2]https://huggingface.co/spaces/MLSpeech/CarelessWhisper-low-latency-streaming

II. RELATED WORK

A wide range of streaming ASR methods have been developed over the years. One of the most prominent architectures is the recurrent neural network transducer (RNN-T) [7], which has been widely adopted in efforts to enable streaming recognition. The RNN-T model typically comprises a long short-term memory (LSTM) network [11] and a bidirectional recurrent neural network (RNN) [34]. Due to the inherently causal nature of recurrent architectures, RNN-T is well-suited for streaming applications.

Kurata *et al.* [17] use knowledge distillation to transfer information from an offline teacher model to a streaming student model based on RNN-T. Rao *et al.* [30] propose an RNN-T architecture that predicts word-pieces rather than individual characters, while adding pronunciation data to improve performance. He *et al.* [9] design an RNN-T model optimized for mobile devices by applying quantization and optimizing inference efficiency.

An alternative approach is the Transformer Transducer [44], which replaces the recurrent components of the RNN-T with a Transformer encoder. Tripathi *et al.* [36] present a Transformer Transducer capable of handling both online and offline transcription, using a hybrid architecture that fuses two types of Transformer encoders—one with causal masking and one without. Chen *et al.* [3] apply chunk-wise attention with causal masking, while using an LSTM as the prediction network. Zhang *et al.* [45] propose a similar architecture to that of Tripathi *et al.*, with minor modifications to the encoder's feedforward layers. Kumar *et al.* [16] integrate a self-supervised pre-trained model as the transducer encoder, allowing for rapid adaptation of existing models to streaming scenarios.

Recent efforts have also explored Transformer-based models directly for streaming ASR [39]. Moritz *et al.* [25] combine a Transformer encoder with a CTC head and a triggered attention [26] decoder. Moritz *et al.* [27] propose a dual causal/non-causal self-attention mechanism in conjunction with a triggered-attention [26] decoder, yielding a dual ASR model. Other works [2], [37] investigate decoder-only Transformer architectures, which naturally fit the streaming paradigm due to the causal nature of the Transformer decoder. Shi *et al.* [35] introduce the Emformer, an enhanced version of the augmented memory Transformer from Wu *et al.* [43]. Wang *et al.* [40] train a Transformer encoder to detect word boundaries using forced alignment [24]. Jia *et al.* [15] propose a SpeechLLM method that interleaves audio and text embeddings into a large language model (LLM) decoder, trained on a CTC-aligned dataset, while limiting the past context window. Choi *et al.* [4] fine-tune self-supervised speech models (S3Ms), exploring different masking strategies to adapt the models to streaming. Tsunoo *et al.* [38] propose an encoder-decoder Transformer trained via knowledge distillation [10], [18], [22]. To enhance transcription quality, they introduce block-wise synchronous beam search combined with block boundary detection techniques.

Although the Whisper model [29] was not designed for streaming—due to the non-causal nature of its encoder within the encoder-decoder framework—several studies have attempted to overcome this limitation. Macháček *et al.* [23] avoid fine-tuning by using an audio buffer as input and emit transcriptions only after complete utterances are formed, applying local agreement [20] between sub-utterances. Similarly, Wang *et al.* [41] also forgo fine-tuning by developing a heuristic based on Whisper alignment heads and using a truncation detection module to determine when to emit tokens. Although these approaches do not require training, the truncation detection module must be trained separately. Moreover, both methods suffer from inefficiencies, as they require padding each buffer input to the full context length of the model, resulting in unnecessary computation.

Wang *et al.* [42] propose training Whisper to detect a designated hush-word at the end of each chunk, enabling the model to stop decoding appropriately. They also introduce a hybrid CPU/GPU pipeline that offloads most of the decoding process to idle CPU resources. This approach does not require input padding to the full context length for each chunk. Zhou *et al.* [46] propose training a new CTC head on top of the Whisper encoder, which is fine-tuned using a causal mask to make the encoder output compatible with streaming input. In this method, inference is conducted in two passes: the CTC head predicts the most probable next token, and the Whisper decoder ranks the candidate hypotheses.

While there is a growing body of work aimed at adapting pre-trained models such as Whisper for streaming applications, existing approaches have notable limitations. Some do not achieve true streaming behavior, while others introduce high computational overhead. Furthermore, approaches such as those proposed by Zhou *et al.* [46] and Wang *et al.* [42] require modifications to the model architecture or fine-tuning of the entire model, leading to a substantial increase in the number of parameters needed specifically for streaming tasks, in addition to the original Whisper model.

III. PROBLEM SETUP

We start by describing an encoder-decoder Transformer-based ASR model, such as Whisper [29]. It consists of a front-end composed of a few CNN layers, a transformer encoder, and a transformer decoder. The model receives the log-mel spectrogram a feature representation of speech as input. The input passes through a CNN layer that narrows the time dimension. Denote $\mathbf{X}_T = (\mathbf{x}_1, \ldots \mathbf{x}_T)$ the output sequence from the front-end, which serves as input to the transformer encoder, where T is the duration of the front-end sequence, and $\mathbf{x}_t \in \mathbb{R}^d$ for $1 \leq t \leq T$. The encoder maps the front-end sequence to a sequence of representations $\mathbf{Z}_T = (\mathbf{z}_1, \ldots, \mathbf{z}_T)$:

$$\text{Encoder}(\mathbf{X}_T) = \mathbf{Z}_T \ . \qquad (1)$$

Where $\mathbf{z}_t \in \mathbb{R}^d$ for $1 \leq t \leq T$. The decoder receives as input the representations from the encoder and predicts the probability distribution over the possible set of tokens, $\mathcal{V}$, auto-regressively. We denote by $\hat{\mathbf{y}}_{<i}$ the vector of all previous tokens, $\hat{\mathbf{y}}_{<i} = (\hat{y}_1, \ldots, \hat{y}_{i-1})$. Formally, the decoder predicts the conditional probability of the next token $\hat{y}_i \in \mathcal{V}$ given all previous tokens and the representations:

$$\text{Decoder}(\mathbf{Z}_T, \hat{\mathbf{y}}_{<i}) = P(\hat{y}_i | \hat{\mathbf{y}}_{<i}, \mathbf{Z}_T) \ . \qquad (2)$$

For ease of notation, we will use the notations $P(y_i|\hat{\mathbf{y}}_{<i}, \mathbf{Z}_T)$ and $P(y_i|\hat{\mathbf{y}}_{<i}, \mathbf{X}_T)$ interchangeably, where they both refer to the same distribution. In the case of greedy decoding, the predicted token is the one that maximizes the decoder output:

$$v_i^* = \arg\max_{v \in \mathcal{V}} P(\hat{y}_i = v | \hat{\mathbf{y}}_{<i}, \mathbf{Z}_T) \qquad (3)$$

The non-streaming encoder operates on a fixed number of frames T as input (e.g., the input to all Whisper models, which is composed of $T = 1500$ frames). During streaming, the ASR system processes a *chunk* of speech composed of τ frames (which correspond to τ vectors of the encoder representation). That is, τ defines the resolution at which streaming occurs. More precisely, the k-th chunk is represented as $\mathbf{X}_{(k-1)\tau}^{k\tau} = (\mathbf{x}_{(k-1)\tau}, \mathbf{x}_{(k-1)\tau+1}, \ldots, \mathbf{x}_{k\tau-1})$. The *streaming encoder* operates on one such chunk at a time, producing the corresponding sequence of representations. Consequently, the input chunk $\mathbf{X}_{(k-1)\tau}^{k\tau}$ yields the output $\tilde{\mathbf{Z}}_{(k-1)\tau}^{k\tau}$. As we will show, this sequence $\tilde{\mathbf{Z}}_{(k-1)\tau}^{k\tau}$ differs from the subsequence $\mathbf{Z}_{(k-1)\tau}^{k\tau}$, which would result from encoding the entire front-end output $\mathbf{X}_T$ and then selecting the relevant portion spanning $(k-1)\tau$ to $k\tau$. This discrepancy motivates our use of distinct notation for these two sequences. We denote the streaming encoder for input of duration τ as follows:

$$\text{StreamingEncoder}(\mathbf{X}_{(k-1)\tau}^{k\tau}) = \tilde{\mathbf{Z}}_{(k-1)\tau}^{k\tau} . \qquad (4)$$

The streaming encoder attends to the current chunk as well as previous cached chunks when calculating the representation $\tilde{\mathbf{Z}}_{(k-1)\tau}^{k\tau}$ for the newly arrived frames $\mathbf{X}_{(k-1)\tau}^{k\tau}$.

The streaming decoder gets as input the hidden state subsequence $\tilde{\mathbf{Z}}_{(k-1)\tau}^{k\tau}$ and predicts auto-regressively the probability of the next token $\tilde{y}_i \in \mathcal{V}$ given the previous predicted tokens $\tilde{\mathbf{y}}_{<i} = (\tilde{y}_1, \ldots, \tilde{y}_{i-1})$:

$$\text{StreamingDecoder}(\tilde{\mathbf{Z}}_{(k-1)\tau}^{k\tau}, \tilde{\mathbf{y}}_{<i}) = P(\tilde{y}_i | \tilde{\mathbf{y}}_{<i}, \tilde{\mathbf{Z}}_{(k-1)\tau}^{k\tau}) . \qquad (5)$$

Note that when the streaming decoder calculate the probability distribution of the next token, it attends to $\mathbf{Z}_{(k-1)\tau}^{k\tau}$ as well as to the cached values of the previous given features $\mathbf{Z}_1^{(k-1)\tau}$.

Our goal is to design and implement a streaming encoder and decoder. They will be fine-tuned using existing pretrained model weights, with the objective that the overall performance of the streaming ASR will be comparable to that of the offline ASR. Formally, denote by $\mathbf{X}_{k\tau}$ the input up to time frame $k\tau$, that is, $\mathbf{X}_{k\tau} = \mathbf{X}_1^{k\tau}$, and denote by $\mathbf{y}_{k\tau}$ the corresponding ground truth token sequence. Similarly, denote $\hat{\mathbf{y}}_{k\tau}$ and $\tilde{\mathbf{y}}_{k\tau}$ the predicted token sequence of the offline and the streaming decoder, respectively. We aim that the word error rate (WER) of the streaming decoder $\text{WER}(\tilde{\mathbf{y}}_{k\tau}, \mathbf{y}_{k\tau})$ is low and comparable to $\text{WER}(\hat{\mathbf{y}}_{k\tau}, \mathbf{y}_{k\tau})$.

IV. METHOD

Originally, the transformer encoder utilizes non-causal self-attention mechanism [39]. The encoder is composed of L self-attention (SA) layers. Each SA layer l receives an input $\mathbf{U}_T^{l-1}$ from the previous layer $l-1$, where $\mathbf{U}_T^0 = \mathbf{X}_T$, and T is the total number of frames in the input. It outputs the queries $\mathbf{Q} \in \mathbb{R}^{T \times d}$, the keys $\mathbf{K} \in \mathbb{R}^{T \times d}$, and values $\mathbf{V} \in \mathbb{R}^{T \times d}$,

where d denotes the vector dimension. Specifically, the queries, keys, and values are all calculated using the same $\mathbf{U}_T$:

$$\mathbf{Q}_T^l = \mathbf{U}_T^l \mathbf{W}_Q^l, \quad \mathbf{K}_T^l = \mathbf{U}_T^l \mathbf{W}_K^l, \quad \mathbf{V}_T^l = \mathbf{U}_T^l \mathbf{W}_V^l , \quad (6)$$

where $\mathbf{W}_Q^l, \mathbf{W}_K^l, \mathbf{W}_V^l \in \mathbb{R}^{d \times d}$ are learned matrices for layer l. The *self-attention* is defined as

$$\text{SA}^l(\mathbf{U}_T^l) = \text{Softmax}\left(\frac{\mathbf{Q}_T^l \mathbf{K}_T^{l\top}}{\sqrt{d}}\right) \mathbf{V}_T^l . \qquad (7)$$

After the self-attention layer, a feed-forward (FF) layer is then applied using a residual connection. Thus, given an activation function f, one layer of the encoder can be described as:

$$\mathbf{U}^l = f\left(\mathbf{W}^l(\text{SA}^l(\mathbf{U}^{l-1}) + \mathbf{U}^{l-1}) + \mathbf{b}^l\right) . \qquad (8)$$

where $\mathbf{W}^l \in \mathbb{R}^{d \times d}$ and $\mathbf{b}^l \in \mathbb{R}^d$ are the FF learned parameters. The speech representation is the outout of the last encoder layer L:

$$\mathbf{Z}_T = \text{Encoder}(\mathbf{X}_T) \qquad (9)$$

To transform the encoder into a causal encoder, one can feed the speech signal incrementally with $k\tau$ frames at each step ($k\tau < T$). Our key observation is that when only the first k frames of the input are provided, the encoder produces a representation $\tilde{\mathbf{Z}}_{k\tau}$ that differs from the first $k\tau$ vectors of $\mathbf{Z}_T$. We show that formally in the following theorem.

Theorem 1. *Let $k\tau < T$, where k is the frame index and τ is the chunk size. Denote by $\mathbf{X}_T$, and by $\mathbf{X}_{k\tau}$ the full and the truncated inputs to the encoder, respectively. Let $\mathbf{Z}_T = \text{Encoder}(\mathbf{X}_T)$ and let $\mathbf{Z}_{k\tau} = \text{Encoder}(\mathbf{X}_{k\tau})$. Then*

$$[\mathbf{Z}_T]_t \neq [\mathbf{Z}_{k\tau}]_t \quad 1 \leq t \leq k\tau , \qquad (10)$$

where $[\mathbf{Z}_T]_t$ is the t-th representation.

The proof of the theorem can be found in Appendix A. According to this theorem the encoder is designed and trained to work in a non-causal form. We convert it to be a causal by fine-tuning. During training a causal mask is applied on the self-attention weights of the encoder in all its layers, utilizing the same concept that is used in training the causal decoder.

A. Streaming Encoder

We start by defining a *mask matrix* that will be added to the self-attention matrix. Elements in the matrix that correspond to no masking are assigned to be 0 whereas the elements that are masked are assigned the value of $-\infty$. We define two parameters of the masking. Let T be the maximal context available on the encoder's input. Let $\tau < T$ be the chunk size or the granularity of encoder frames, and $k \in \mathbb{N}$ the chunk index. In our setting the first chunk is larger than subsequent chunks, and $\tau_0 < T$ denotes its size. The elements of the mask matrix are defined as follows

$$\mathbf{M}_{ij}(k, \tau, \tau_0) = \begin{cases} 0 & \lceil \frac{i}{\tau} \rceil \geq \lceil \frac{j}{\tau} \rceil \vee (i,j) \in [1, \tau_0] \times [1, \tau_0] \\ -\infty & \text{otherwise} \end{cases}$$
$$(11)$$

We exemplify this notation using Figure 1, where we assume a chunk size of $\tau = 15$ frames, an initial chunk size of $\tau_0 =$
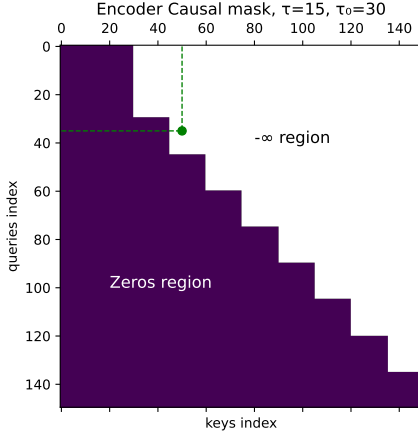
Fig. 1: Encoder causal mask example, $\tau = 15, \tau_0 = 30$ given $k = 10$ chunks. Such mask applies that the model waits 600 msec for the first buffer before feeding the input to the encoder. Then, input is being fed every 300 msec. Purple regions contain zeros while white regions contain $-\infty$. The index (35,50) is marked in a green point.

30 frames, and that the model is currently processing chunk number $k = 10$. Let's examine the element on the mask matrix. Consider the 35-th row of the matrix. Elements "inside" the chunk are not masked, so for the element $(i = 35, j = 23)$: $\left\lceil \frac{35}{15} \right\rceil = 3 \geq \left\lceil \frac{23}{15} \right\rceil = 2$. Whereas elements outsize the chunk, should be masked. For example, for $(i = 35, j = 50)$, we have $\left\lceil \frac{35}{15} \right\rceil = 3 < \left\lceil \frac{50}{15} \right\rceil = 4$.

The mask $\mathbf{M}(k, \tau, \tau_0) \in \{0, -\infty\}^{k\tau \times k\tau}$ is applied to the dot product in the following way:

$$\widetilde{\mathrm{SA}}(\mathbf{X}_{k\tau}, \tau, \tau_0) = \mathrm{Softmax}\left(\frac{\mathbf{Q}_{k\tau} \mathbf{K}_{k\tau}^\top + \mathbf{M}(k, \tau, \tau_0)}{\sqrt{d}} \right) \mathbf{V}_{k\tau} \tag{12}$$

Here we omitted the layer super-script, and (12) refers to any of the encoder layers. With this masked self-attention mechanism, the encoder's representation of the first $k\tau$ frames remains unchanged whether processing is performed chunk by chunk up to chunk k or over the entire input sequence at once, as formalized in the following theorem.

Theorem 2. *Let $k\tau < T$, where k is the chunk index and τ is the chunk size. Denote by $\mathbf{X}_T$, and by $\mathbf{X}_{k\tau}$ the full and the truncated inputs to the encoder respectively. Let $\tilde{\mathbf{Z}}_T = \mathrm{StreamingEncoder}(\mathbf{X}_T)$ and let $\tilde{\mathbf{Z}}_{k\tau} = \mathrm{StreamingEncoder}(\mathbf{X}_{k\tau})$. Then*

$$[\tilde{\mathbf{Z}}_T]_t = [\tilde{\mathbf{Z}}_{k\tau}]_t \quad 1 \leq t \leq k\tau \tag{13}$$

where $[\tilde{\mathbf{Z}}_T]_t$ is the t-th representation.

The proof of the theorem is given in Appendix A. In other words, employing this causal mask enables the encoder to perform a forward pass at each iteration solely over the newly arrived frames, eliminating the need to recompute the full self-attention over the entire sequence each time.

To summarize, we propose to replace the non-causal encoder with a causal encoder by adding causal masking to each of the SA layers, and then fine-tune it.

B. Streaming Decoder

The streaming decoder receives the encoded speech representation of the last chunk $\tilde{\mathbf{Z}}_{(k-1)\tau}^{k\tau}$ from the streaming encoder. The decoder has a caching mechanism so it keeps the representation of previous chunks. As it operates in a auto-regressive manner it also gets as input its previous predicted tokens, and its goal is to predict the distribution of the next token as in (2). To achieve this, the decoder employs a cross-attention layer. While cross-attention operates using the same mechanism as self-attention, it differs in the way queries, keys, and values are constructed. Specifically, the queries are derived from the output of the decoder self-attention layers up-to the previous token, denoted as $\bar{\mathbf{U}}_{<i}^l$, while the keys and values come from the acoustic feature representations $\tilde{\mathbf{Z}}_{k\tau}$. Thus, a cross-attention layer is defined as follows:

$$\mathbf{Q}_{<i}^l = \bar{\mathbf{U}}_{<i}^l \bar{\mathbf{W}}_Q^l, \quad \mathbf{K}_{k\tau}^l = \tilde{\mathbf{Z}}_{k\tau} \bar{\mathbf{W}}_K^l, \quad \mathbf{V}_{k\tau}^l = \tilde{\mathbf{Z}}_{k\tau} \bar{\mathbf{W}}_V^l \tag{14}$$

where $\bar{\mathbf{W}}_Q^l, \bar{\mathbf{W}}_K^l, \bar{\mathbf{W}}_V^l \in \mathbb{R}^{d \times d}$ are learned matrices for layer l of the decoder. The *cross-attention* is defined as

$$\mathrm{CA}^l(\bar{\mathbf{U}}_{<i}^l, \tilde{\mathbf{Z}}_{k\tau}) = \mathrm{Softmax}\left(\frac{\mathbf{Q}_{<i}^l \mathbf{K}_{k\tau}^{l\top}}{\sqrt{d}} \right) \mathbf{V}_{k\tau}^l \tag{15}$$

Overall, the decoder is built from a self-attention layer, a cross-attention layer and a feed-forward layer with residual connections:

$$\mathbf{U}_{<i}^l = f\Bigg(\mathbf{W}^l \Big(\mathrm{CA}^l\big(\mathrm{SA}^l(\mathbf{U}_{<i}^{l-1}) + \mathbf{U}_{<i}^{l-1}, \tilde{\mathbf{Z}}_{k\tau} \big)$$
$$+ \mathrm{SA}^l(\mathbf{U}_{<i}^{l-1}, \tilde{\mathbf{Z}}_{k\tau}) \Big) + \mathbf{b}^l \Bigg), \tag{16}$$

where $\mathbf{U}_{<i}^{l-1}$ denotes the representation of the input token sequence $\mathbf{y}_{<i}$ after $l - 1$ layers, and $\mathrm{SA}(\cdot)$ is defined in (7).

Unlike the non-streaming decoder, such as the one implemented in the Whisper model, which expects a full feature matrix of shape $T \times d$, a streaming decoder operates incrementally, processing acoustic inputs of shape $k\tau \times d$ as they arrive, enabling token prediction in a streaming manner.

To summarize, the propose streaming decoder maintains a caching mechanism to handle the streaming input. Moreover, the steaming decoder undergoes a fine-tune together with the streaming encoder as will be detailed in the next sections.

C. Streaming Inference

Decoding the optimal token sequence is typically framed as predicting the most probable token

$$v_i^* = \arg\max_{v \in \mathcal{V}} P(\hat{y}_i = v | \hat{\mathbf{y}}_{<i}, \mathbf{Z}_T) . \tag{17}$$

Throughout this paper, we primarily use the *max* operation to represent *greedy decoding*, where the token with the highest conditional probability is selected at each step. While it is possible to *sample* tokens from the probability distribution instead, this alternative is only considered in the context of *beam search* decoding.

Applying (17) in the streaming setting is challenging, particularly when processing fixed-size input chunks that are not
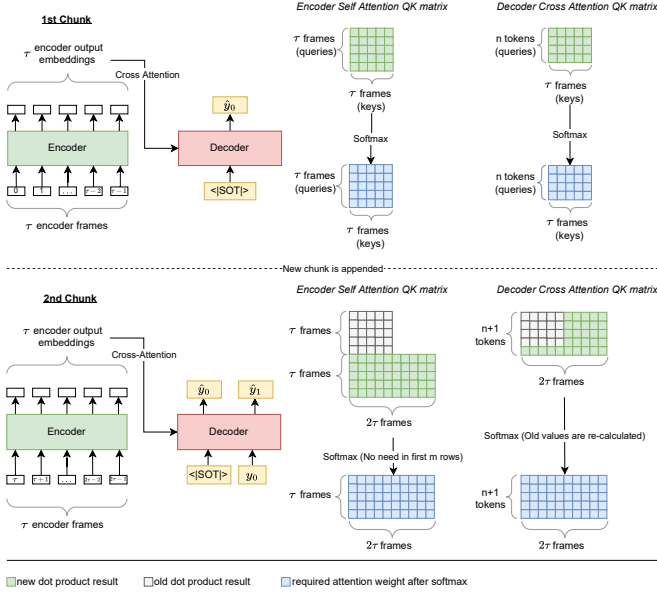
Fig. 2: The inference process, using a chunk size of τ, initial chunk of size $\tau_0 = \tau$. The figure also illustrates how attention weight matrices are computed, specifically, within the encoder's self-attention and the decoder's cross-attention mechanisms.

necessarily aligned with token boundaries. This setup introduces two primary obstacles. First, a token may be *partially* contained within a chunk, with the remainder spanning into the next one. In such cases, the model lacks sufficient information to confidently predict the complete token. Second, the chunk may not provide enough contextual information, leading to premature or unstable token predictions that would differ if future input were available, especially for tokens with similar phonetic content. These challenges underscore the need to explicitly address temporal boundaries and ensure contextual continuity during streaming inference—considerations that motivate our focus in both inference design and fine-tuning, as we elaborate in this and subsequent sections.

To overcome these obstacles, we propose a decoding mechanism that supports token-level regression, allowing the decoder to revise past predictions in light of new information.

A token is considered *stable* if its prediction is consistent across two consecutive chunks. When this condition is met, the prediction is considered finalized. In contrast, *unstable* tokens—those with inconsistent predictions—are discarded, and decoding is resumed from the first unstable position. We describe this heuristic in the context of both greedy decoding and beam search decoding.

1) Greedy Streaming Decoding: Greedy decoding is a decoding strategy in which, at each time step, the model selects the token with the highest predicted probability, without considering alternative candidates. We start with a definition of a *stable token* for greedy decoding.

Definition 1 (Stable Token for Greedy Decoding). *A token $y_i = v$ predicted in the k-th chunk is said to be stable under greedy decoding if it satisfies at least one of the following conditions. Either the token v has a greater or equal probability*

given a new chunk relative to the previous chunk:

$$P(y_i = v \mid \mathbf{y}_{<i}, \mathbf{X}_{k\tau}) \geq P(y_i = v \mid \mathbf{y}_{<i}, \mathbf{X}_{(k-1)\tau}) \quad (18)$$

or v is the most probable token given the new chunk:

$$v = \arg\max_{u \in \mathcal{V}} P(y_i = u \mid \mathbf{y}_{<i}, \mathbf{X}_{k\tau}) \ . \quad (19)$$

A token is considered stable as long as it remains the most probable token in the distribution. Additionally, a token may be marked as stable even if it is not the most probable token, as long as its probability increases.

The greedy decoding algorithm is modified as follows: upon the arrival of a new chunk k, the prediction of token i proceeds only if all of the last n tokens have been verified as stable. Otherwise, the decoding process is resumed from the first unstable token, discarding any subsequent tokens. The complete greedy streaming decoding process is presented in Algorithm 1.

Algorithm 1 Streaming Greedy Decoding

1: **Input:** n
2: **Output:** $\hat{\mathbf{y}}$
3: $\hat{\mathbf{y}} \leftarrow \varnothing$
4: completed $\leftarrow$ False
5: **for** $k \in \{0, \ldots, \frac{T}{\tau}\}$ **do**
6:     new_chunk $\leftarrow$ True
7:     **while** not completed **do**
8:         **if** new_chunk **then**
9:             new_chunk $\leftarrow$ False
            // *Check for unstable tokens*
10:             **for** $m \in \{n-1, n-2, \ldots, 0\}$ **do**
11:                 **if** token y_{i-m} is unstable **then**
12:                     $\hat{\mathbf{y}} \leftarrow \hat{\mathbf{y}}_{<i-m}$
13:                     **break**
14:                 **end if**
15:             **end for**
16:         **end if**
        // *Decode greedily*
17:         $\hat{\mathbf{y}} \leftarrow \hat{\mathbf{y}}_{<i-m} \oplus \arg\max P(\hat{y}_{i-m} \mid \hat{\mathbf{y}}_{<i-m}, \mathbf{X}_{k\tau})$
18:         completed $\leftarrow EOT \in \hat{\mathbf{y}}$
19:     **end while**
20: **end for**
21: **return** $\hat{\mathbf{y}}$

The next theorem states that our proposed greedy decoding will have at least a locally optimal token prediction, given that the probability $P(y_i \mid \mathbf{y}_{<i}, \mathbf{X}_{k\tau})$ was correctly estimated.

Theorem 3 (Streaming Greedy Decoding Optimality). *Let*

$$P^*(y_i \mid \mathbf{y}_{<i}, \mathbf{X}_{k\tau}) \quad (20)$$

be the optimal probability distribution of the i-th token given the preceding tokens, and the acoustic data till $k\tau$. Denote by ρ_k the probability path of the predicted token sequence until the chunk k. Our proposed greedy decoding algorithm, as depicted on Algorithm 1, is optimal in the sense that it yields a probability path ρ_k^{CW} which is larger or equal on the probability path of the greedy algorithm, ρ_k^G.

The theorem is proven by induction and is included in Appendix A.

2) Beam-Search Streaming Decoding: Beam search decoding is a heuristic search algorithm that explores multiple hypotheses at each time step, maintaining the top-scoring sequences within a fixed-size beam to balance between accuracy and computational efficiency. We enhance the beam search decoding process by adding a stability check on the last n tokens when a new chunk arrives. Let b denote the beam size. A token is considered stable if and only if it remains within the top-b candidates (i.e., within the beam) after incorporating the latest acoustic frame.

We define the operator TopK as follows.

Definition 2 (Top-k Operator). *Let $\mathbf{p} \in \mathbb{R}^{|\mathcal{V}|}$ be a vector of real-valued scores indexed over a finite set $\mathcal{V}$. The Top-k operator, denoted by $\mathrm{TopK}(\mathbf{p}, k)$, returns the set of indices corresponding to the k largest values in $\mathbf{p}$:*

$$\mathrm{TopK}(\mathbf{p}, k) = \{j \in \mathcal{V} \mid j \text{ is among the } k \text{ largest entries of } \mathbf{p}\}. \tag{21}$$

Now we can define a stable token for the beam search decoding.

Definition 3 (Stable Token for Beam Search Decoding). *A token $y_i = v$ is defined to be* stable *under beam search decoding if it satisfies:*

$$v \in \mathrm{TopK}\left(P(y_i \mid \mathbf{y}_{<i}, \mathbf{X}_{k\tau}), b\right) \tag{22}$$

That is, the token is stable if it remains within the top-b most probable candidates at its position in the current beam step.

Unlike greedy decoding, where a single prediction path is followed, beam search maintains multiple hypotheses in parallel. Typically, decoding is considered complete only once a sufficient number of hypotheses have terminated, i.e., their final token is the end-of-transcription (*E*OT) symbol. However, in the streaming setting, this approach can introduce errors such as hallucinations or repeated phrases. This often occurs because the input buffer may end mid-word, leading some beams to favor repetitive completions or hallucinated content rather than emitting *E*OT. To mitigate this, we adopt a greedy-style stopping criterion: if any hypothesis within the beam predicts an *E*OT token, the decoding is paused until the next acoustic frame is received.

The full beam search algorithm is available on Algorithm 2. Note that the suggested version of beam search decoding involves a varying length of beams during the decoding process, since the stability check per token might yield different regression indices.

D. Word Level Timestamps

Recall that our setting is designed to address temporal boundaries and maintain contextual continuity during streaming inference. An important byproduct of tackling this challenge is a stronger correspondence between the predicted decoder tokens and the underlying encoder representation, which can be leveraged to develop a more effective token-to-acoustic alignment mechanism.

This behavior is illustrated in Figure 3, where the X-axis represents the top-5 token predictions and the Y-axis indicates

---

Algorithm 2 Streaming Beam Search Decoding

1: **Input:** n, b
2: **Output:** $\hat{\mathbf{y}}$
   // Initialize beam
3: $\mathcal{B} \leftarrow \varnothing$
4: completed $\leftarrow$ False
5: **for** $k \in \{0, \dots, \frac{T}{\tau}\}$ **do**
6:    new_chunk $\leftarrow$ True
7:    **while** not completed **do**
8:       **for** $\mathbf{y} \in \mathcal{B}$ **do**
9:          **if** new_chunk **then**
10:           new_chunk $\leftarrow$ False
              // Check for unstable tokens
11:           **for** $m \in \{n-1, n-2, \dots, 0\}$ **do**
12:             **if** token y_{i-m} is unstable **then**
13:               $\hat{\mathbf{y}} \leftarrow \mathbf{y}_{<i-m}$
14:               **break**
15:             **end if**
16:           **end for**
17:          **end if**
             // Decode with beam-search
18:          **for** $t \in \mathrm{TopK}\left(\log P(\hat{y}_{i-m} \mid \hat{\mathbf{y}}_{<i-m}, \mathbf{X}_{k\tau}), b\right)$ **do**
19:            $\tilde{\mathbf{y}} \leftarrow \hat{\mathbf{y}} \oplus t$
20:            $\mathcal{B} \leftarrow \mathcal{B} \cup \tilde{\mathbf{y}}$
21:          **end for**
22:       **end for**
          // Store in beam top b hypotheses
23:       $\mathcal{B} \leftarrow \mathrm{TopK}(\mathcal{B}, b)$
24:       completed $\leftarrow$ EOT $\in \mathcal{B}$
25:    **end while**
26: **end for**
27: **return** $\mathbf{y}$ - the most probable token sequence in $\mathcal{B}$

---

the number of processed acoustic frames. The fine-tuned CarelessWhisper model (right plot) demonstrates increased confidence in the correct token as more acoustic context becomes available, in contrast to the untrained Whisper model (left plot). Specifically, the fine-tuned model begins to predict the correct token `your` one frame earlier than its untrained counterpart.

Based on this observation, we propose a simple method for generating online word-level timestamps, described in Algorithm 4. The algorithm's core idea is straightforward: if the model predicts any token other than the *E*OT token, it indicates the recognition of a new word. The current timestamp is then assigned to this new word. In this way, the end of the previous word is implicitly defined by the start time of the next predicted word—creating a consistent, streaming-aligned segmentation. Note that this method is applicable only to models fine-tuned to work with a chunk size of 40 msec or 100 msec. Larger chunk sizes may span multiple words, making precise word boundaries ambiguous. We demonstrate the effectiveness of the resulted timestamps in Section VII.

V. EFFICIENCY

Before turning to empirical evaluation of our proposed method we present efficiency consideration and implementation

Whisper: '$P(y_3|y_{<3}, X_\tau)$' - correct token: `your`

τ[samples]	0	1	2	3	4
1600	<EOT>	a	to	.	the
3200	<EOT>	a	to	.	the
4800	<EOT>	a	to	.	the
6400	<EOT>	a	to	.	the
8000	<EOT>	a	to	.	the
9600	<EOT>	a	to	her	it
11200	<EOT>	your	her	you	to
12800	your	<EOT>	you	her	a
14400	your	<EOT>	you	her	to
16000	your	<EOT>	you	her	,

Sorted tokens (Descending)

Causal Whisper: '$P(y_3|y_{<3}, X_\tau)$' - correct token: `your`

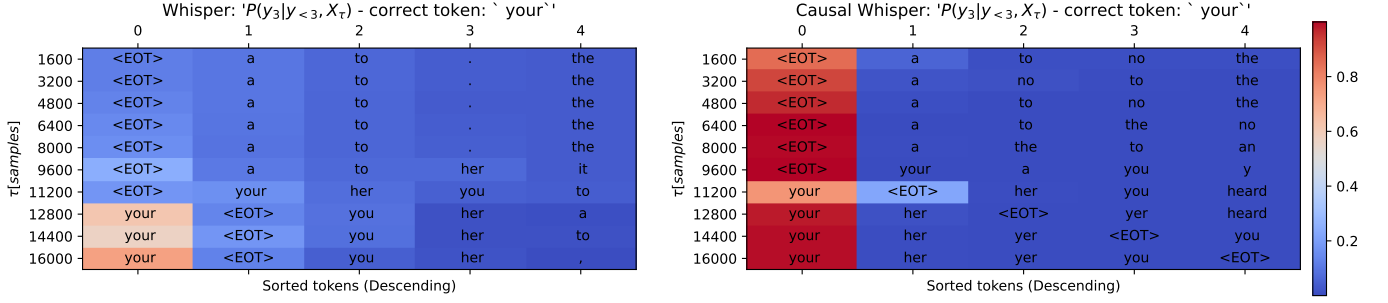| τ[samples]	0	1	2	3	4
1600	<EOT>	a	to	no	the
3200	<EOT>	a	no	to	the
4800	<EOT>	a	to	no	the
6400	<EOT>	a	to	the	no
8000	<EOT>	a	the	to	an
9600	<EOT>	your	a	you	y
11200	your	<EOT>	her	you	heard
12800	your	her	<EOT>	yer	heard
14400	your	her	yer	<EOT>	you
16000	your	her	yer	you	<EOT>

Sorted tokens (Descending)

Fig. 3: Token distribution for the Whisper model (left) and CarelessWhisper (right) for third token over time, conditioned on the ground truth prefix '*she had.*' The full utterance is: "*she had your dark suit in greasy wash water all year.*" The plots show the probability distribution of the **third** token, rather than the sequence of predicted tokens. As such, *EOT* is predicted token as long as there is sufficient acoustic evidence to predict '*your.*' Hence, the token '*had*' does not appear before the token '*your.*'

of KV-cache both for the encoder and the decoder. We then state the complexity of the proposed algorithm.

A. KV-Cache: Encoder

When using causal self-attention, the encoder's computation can be optimized through a KV-cache mechanism. Because new acoustic frames depend only on the current chunk and past inputs, the key and value matrices ($\mathbf{K}$, $\mathbf{V}$) at each layer can be cached rather than recomputed at every iteration—similar to the caching strategy used in causal decoders.

By design, the output of the encoder at position t is influenced only by the t-th row of the self-attention weights matrix. When applying a causal mask, each encoder output at index t is conditioned solely on the current and preceding chunks. As a result, previously computed matrices $\mathbf{K}$ and $\mathbf{V}$ remain valid for future steps and can be reused. This caching mechanism reduces the encoder's computational complexity from quadratic to linear, significantly improving efficiency during streaming inference. A detailed complexity analysis is provided in Section V-C.

B. KV-Cache: Decoder

The decoder incorporates two distinct attention mechanisms: self-attention and cross-attention—each with its own KV-cache policy.

a) Cross-Attention KV-Cache: As discussed in Section V-A and formalized in Theorem 2, encoder outputs corresponding to past acoustic frames are independent of future inputs. Therefore, when a new audio chunk arrives, the decoder computes $\mathbf{K}$ and $\mathbf{V}$ values only for this new chunk. Previously processed chunks are stored and reused. The dot product between the new query and the cached key-value pairs is then calculated as usual. This mechanism defines the cross-attention KV-cache and enables significant computational savings during streaming.

b) Self-Attention KV-Cache: In contrast to cross-attention cache, caching self-attention activations in the decoder is less straightforward. This is due to the dynamic nature of the decoder's input embeddings: each buffer update introduces new acoustic information, which alters the decoder's context and thus the token embeddings.

This distributional drift arises because the decoder continuously receives new audio data. Each decoder layer depends on a causal self-attention block, a cross-attention block, and a feed-forward network. While the self-attention is strictly causal (only attending to past tokens), the cross-attention is not: decoded tokens may attend to future acoustic frames. Importantly, many Whisper cross-attention heads are neither monotonic nor aligned with the token sequence.

To illustrate this effect, consider the t-th token's cross-attention output at two consecutive time steps. Let $\bar{\mathbf{U}}_{<i}$ be the representation of the tokens $< i$, and let $\tilde{\mathbf{Z}}_{k\tau}$ and $\tilde{\mathbf{Z}}_{(k+1)\tau}$ denote the encoder outputs after k and $k+1$ chunks, respectively. The t-th row of the cross-attention output is given by:

$$[\text{CA}(\bar{\mathbf{U}}_{<i}, \mathbf{Z}_{k\tau})]_t = \frac{\sum_{j=1}^{k\tau} \exp\left(\frac{[\mathbf{Q}_{<i}]_t[\mathbf{K}_{k\tau}]_j}{\sqrt{d}}\right)[\mathbf{V}_{k\tau}]_j}{\sum_{j=1}^{k\tau} \exp\left(\frac{[\mathbf{Q}_{<i}]_t[\mathbf{K}_{k\tau}]_j}{\sqrt{d}}\right)}$$

(23)

$$[\text{CA}(\bar{\mathbf{U}}_{<i}, \mathbf{Z}_{(k+1)\tau})]_t = \frac{\sum_{j=1}^{(k+1)\tau} \exp\left(\frac{[\mathbf{Q}_{<i}]_t[\mathbf{K}_{(k+1)\tau}]_j}{\sqrt{d}}\right)[\mathbf{V}_{(k+1)\tau}]_j}{\sum_{j=1}^{(k+1)\tau} \exp\left(\frac{[\mathbf{Q}_{<i}]_t[\mathbf{K}_{(k+1)\tau}]_j}{\sqrt{d}}\right)}$$

(24)

Unless the dot-product terms from indices $k\tau + 1$ to $(k+1)\tau$ are exactly zero, we observe that:

$$\left\|\text{CA}(\bar{\mathbf{U}}_{<i}, \mathbf{Z}_{k\tau})_t - \text{CA}(\bar{\mathbf{U}}_{<i}, \mathbf{Z}_{(k+1)\tau})_t\right\|_2 \neq 0 \qquad (25)$$

This shift in the cross-attention output propagates through the model and alters the token embeddings, which in turn affects the self-attention computations in the next layer. Consequently, applying a self-attention KV-cache in the decoder—as done in offline settings—is no longer valid. To address this, we introduce an approximation: from some time index $k\tau < T$, we assume that $\mathbf{K}_{k\tau}^T, \mathbf{V}_{k\tau}^T$ contribute negligibly to subsequent cross-attention computations. Beyond this point, token embeddings are considered stable and can be cached. However, this assumption often fails in practice, as many cross-attention heads are not temporally aligned or monotonic.

Despite this, we propose to empirically examine this approximation to assess whether our fine-tuning method induces more monotonic or stable behavior in the model's attention patterns.

C. Complexity Analysis

Since the proposed streaming Transformer model does not rely on non-causal attention, we conduct a complexity analysis to estimate its computational efficiency advantages.

Theorem 4. *Let T be the input sequence length to the encoder, d the embedding dimension, and τ the chunk size, with $0 < \tau \ll T$. The computation of blocked causal attention over the full sequence during streaming requires $\mathcal{O}(T^2 d + T d^2)$ operations and $\mathcal{O}(Td)$ additional memory.*

The proof is provided in Appendix A. In contrast, methods such as [23], [41], which do not fine-tune Whisper, pad the input signal to the maximum context size whenever a new frame arrives. As a result, the encoder must perform $\mathcal{O}(T^2 d + T d^2)$ operations for each chunk [39]. Given $\frac{T}{\tau}$ chunks, the total encoder-side computational cost becomes $\mathcal{O}\left(\frac{T^3 d}{\tau} + \frac{T^2 d^2}{\tau}\right)$ operations. This difference is expected to have a significant impact, especially in low-latency scenarios where the chunk size is small ($\tau \ll T$). A further demonstration of the runtime advantage appears in Section VII-B.

VI. FINE-TUNING PROCESS

In this section, we describe the fine-tune process. It is depicted in Figure 7 in the Appendix. We define two main objectives for the training process: (1) to adapt the encoder to a causal speech representation, and (2) to teach the decoder when to emit a new token. To address these objectives, we incorporate LoRA layers [13] into the encoder's self-attention layers, as well as into the decoder's self-attention and cross-attention layers. This configuration ensures that only the LoRA components need to be trained, resulting in a compact and efficient module that supports both offline and streaming transcription capabilities. The full fine-tuning algorithm is detailed in Algorithm 3.

To facilitate efficient fine-tuning, we fix a chunk size $\tau \in \mathbb{N}$ such that $0 < \tau \leq T$, where T denotes the maximum encoder context length (determined by the positional embeddings and equal to $T = 1500$ in Whisper [29]). The self-attention mask is defined based on this chunk size τ, and an initial chunk size $0 < \tau_0 \leq T$ is used. Note that while sharing the same mask across all fine-tuning steps increases efficiency, it limits the model's generalization to other chunk sizes. Each chunk is defined in terms of encoder vectors, where each vector corresponds to 20 msec of audio.

A naive adaptation strategy involves evaluating all possible time points at intervals of 20τ msec, denoted by the set I, computing the corresponding target labels using the weak alignment generated via force alignment [24], and back-propagating the loss. Although conceptually straightforward, this method is inefficient due to zero-padding, as many audio samples are shorter than the maximum duration of 30 seconds and thus contain padded regions.

To address this inefficiency, we sample only a subset of the time points in I. Specifically, for each fine-tuning step, we define a sampling fraction $\hat{f} \in (0, 1]$ and randomly select $\hat{f} \cdot |I|$ time points from I, denoted as $\tilde{I}$. We then iterate over this sampled set $\tilde{I}$ during the fine-tuning step. At each fine-tuning

sub-step j, we compute the corresponding target sequence $\mathbf{y}_{<\tilde{I}_j}$ as:

$$\mathbf{y}_{<\tilde{I}_j} = \{y_i \mid t_{\text{end}}(y_i) \leq \tilde{I}_j \text{ sec}\} \qquad (26)$$

Here, $t_{\text{end}}(y_i)$ is the end time of token y_i, determined from the force alignment. For each sub-step, the model is fine-tuned using a cross-entropy loss, $\mathcal{L}_{CE}$, computed over $\mathbf{y}_{<\tilde{I}_j}$ and $\hat{\mathbf{y}}_{<\tilde{I}_j}$.

Algorithm 3 Streaming Whisper LoRA Fine-tuning Process

1: **Input:** Whisper NN - $\mathcal{M}^{LoRA}$, Dataset - $\mathcal{D}$, chunk size τ, initial chunk size τ_0, sample points fraction $\hat{f}$.
2: **for** $\mathcal{B}$ in $\mathcal{D}$ **do**
3:      $\mathbf{X}, \mathbf{y} \leftarrow \mathcal{B}$
4:      $\tilde{I} \leftarrow \text{getSamplePoints}(\tau, \tau_0, \hat{f})$
5:      **for** j in $\{0, 1, \ldots, |\tilde{I}| - 1\}$ **do**
6:          $\hat{\mathbf{y}} \leftarrow \mathcal{M}^{LoRA}(\mathbf{X}_{\tilde{I}_j}, \mathbf{y}_{<j}, \tau, \tau_0)$
7:          $\ell \leftarrow \mathcal{L}_{CE}(\hat{\mathbf{y}}, \mathbf{y})$
8:          calculate_gradients(ℓ)
9:          optimizer_step()
10:      **end for**
11: **end for**

VII. EXPERIMENTS

We refer to our algorithm as *CarelessWhisper*, highlighting it does not care for future context during inference. We evaluate *CarelessWhisper* across several tasks. First, we focus on its primary objective: streaming transcription, assessed using word error rate (WER) and related variants, which we detail below. We then analyze runtime performance using metrics such as Real-Time Factor (RTF) and average latency. Lastly, we evaluate the accuracy of the word-level timestamps generated by the model.

A. Streaming Transcription

We first describe the metrics used to evaluate the performance of different streaming transcription models.

1) Evaluation Metrics: To better assess streaming transcription quality, we employ metrics that are more suitable for streaming scenarios than the standard Word Error Rate (WER).

a) Relative Word Error Rate (RWER): Let $\hat{\mathbf{y}}_\tau$ be the hypothesis generated by the streaming model up until time point τ, containing $\tilde{N}_\tau$ words. Define the set $\hat{\mathcal{Y}} = \{\hat{\mathbf{y}}_0, \ldots, \hat{\mathbf{y}}_T\}$ as the set of hypotheses generated throughout the decoding process. Let $\mathbf{y}$ be the ground-truth transcription, consisting of N words, and let $\mathbf{y}_\tau$ be the prefix of the ground-truth string up to the $\tilde{N}_\tau$-th word. Finally, let I, D, S, and C denote insertions, deletions, substitutions, and correct predictions, respectively. Then, RWER is defined as:

$$\text{RWER}(\mathbf{y}, \hat{\mathcal{Y}}) = \frac{\sum_\tau I(\mathbf{y}_\tau, \hat{\mathbf{y}}_\tau) + D(\mathbf{y}_\tau, \hat{\mathbf{y}}_\tau) + S(\mathbf{y}_\tau, \hat{\mathbf{y}}_\tau)}{\sum_\tau C(\mathbf{y}_\tau, \hat{\mathbf{y}}_\tau) + D(\mathbf{y}_\tau, \hat{\mathbf{y}}_\tau) + S(\mathbf{y}_\tau, \hat{\mathbf{y}}_\tau)}$$

The motivation behind RWER is to evaluate the quality of the partial transcription at each time point, without penalizing for alignment mismatches.

When transcribing streaming audio, the complete transcription must be produced by the end of the stream, while
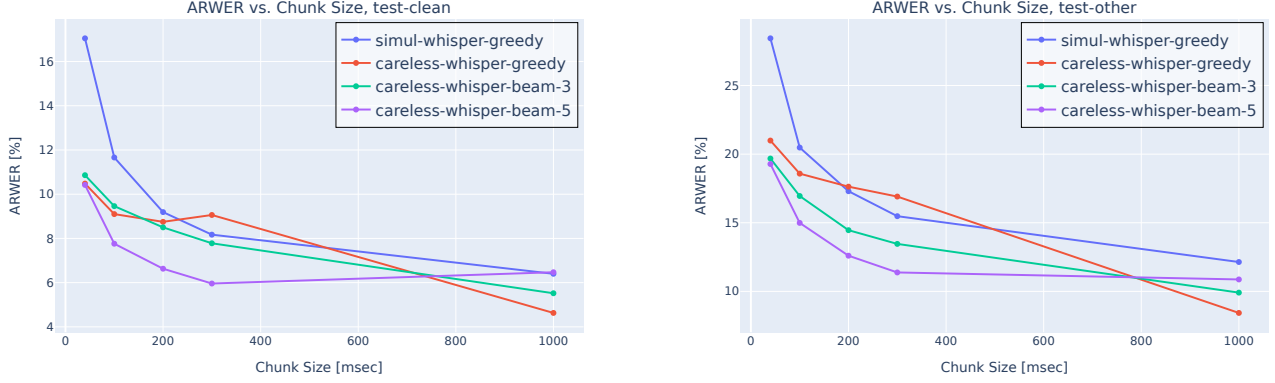
Fig. 4: ARWER vs. Chunk Size per method, on *large-v2* models. Left sub figure presents the results on LibriSpeech test-clean. Right sub figure presents the results on LibriSpeech test-other

minimizing per-word latency. Since RWER does not capture latency or alignment, we introduce an additional metric.

b) Aligned-Relative Word Error Rate (ARWER): The ARWER is defined as:

$$\text{ARWER}(\mathbf{y}, \hat{\mathcal{y}}) = \frac{\sum_\tau I\left(\mathbf{y}_\tau, \hat{\mathbf{y}}_\tau\right) + D\left(\mathbf{y}_\tau, \hat{\mathbf{y}}_\tau\right) + S\left(\mathbf{y}_\tau, \hat{\mathbf{y}}_\tau\right)}{\sum_\tau C\left(\mathbf{y}_\tau, \hat{\mathbf{y}}_\tau\right) + D\left(\mathbf{y}_\tau, \hat{\mathbf{y}}_\tau\right) + S\left(\mathbf{y}_\tau, \hat{\mathbf{y}}_\tau\right)}$$

ARWER is better suited for evaluating transcription quality over time, as it considers alignment between the hypothesis and the ground-truth words that are expected to have been transcribed by each point. Models with higher per-word latency will tend to have higher ARWER, due to increased deletions.

c) Word Error Rate (WER): We also report the standard WER, calculated between the final hypothesis produced at the end of streaming and the full ground-truth transcription.

2) English transcription: For the English transcription task, we fine-tuned three different sizes of the Whisper model: *base*, *small*, and *large-v2*. All models were fine-tuned on the LibriSpeech-train dataset [28], which consists of 960 hours of read speech. The *base* and *small* models were fine-tuned using LoRA layers with a rank of $r = 32$, while the *large-v2* model was fine-tuned with $r = 4$. Fine-tuning was conducted using chunk sizes selected from the set $300, 200, 100, 40$ msec, with an initial chunk size of 600 milliseconds. We used cross-entropy as the loss function and optimized the models with the AdamW optimizer [21], using an initial learning rate of $1e^{-5}$. Full details can be found in Appendix C.

Evaluation was performed on the LibriSpeech *test-clean* and *test-other* datasets. Each fine-tuned model was evaluated on these datasets using both greedy streaming decoding and streaming beam search with beam size $b = 5$ and $n = 2$. We compared our results against *Simul-Whisper* [41] and *Ufal-Whisper* [23], using the same chunk size settings.

Figure 4 presents ARWER results across the different methods. The results indicate that our training approach enhances Whisper's alignment capabilities and outperforms the heuristic approach used in *Simul-Whisper* for both greedy decoding and beam search, except for greedy decoding at a chunk size of 300 ms. When evaluating final transcription quality (Table I) *Simul-Whisper* performs worse than our method on most chunk sizes when using beam search with $b = 5$ and $n = 2$. Results from *Ufal-Whisper* were omitted from Figure 4, as its error rates exceeded 50% for smaller chunk sizes. This suggests that such small chunk sizes are too short for *Ufal-Whisper*, which relies on agreement between utterances.

Complete evaluation results are reported in Table I, where our results are shown using a beam size of $b = 5$ and $n = 2$. The best scores per metric, per dataset, and per chunk size are marked in bold. Overall, our method consistently outperforms competing approaches across most model sizes on both *test-clean* and *test-other* sets.

3) Multilingual Transcription: For the multilingual transcription task, a single *large-v2* model was fine-tuned using a chunk size of 300 msec and an initial chunk size of 600 msec. The training data consisted of the Multilingual LibriSpeech corpus (excluding the English portion), supplemented with the full 960-hour LibriSpeech training set for two epochs. Complete details of the fine-tuning are provided in Appendix C.

Evaluation was conducted on the French, German, Portuguese, and Spanish test subsets of the Multilingual LibriSpeech dataset, using both greedy streaming decoding and streaming beam search with a beam size of $b = 5$ and $n = 2$. We compared our model's performance to that of *Simul-Whisper* and *Ufal-Whisper*, under the same chunking configuration of 300 msec with a 600 msec initial chunk.

As shown in Table II, although our LoRA-fine-tuned model outperforms *Simul-Whisper*, it is consistently outperformed by *Ufal-Whisper* in terms of both WER and ARWER across all evaluated languages. This may be due to the limited multilingual exposure during fine-tuning—unlike the original Whisper model, our fine-tuned version likely does not retain

Model	System		test-clean			test-other		
	Method	Chunk Size (msec)	RWER [%]	ARWER [%]	WER [%]	RWER [%]	ARWER [%]	WER [%]
base	Simul-Whisper [41]	40	27.54	30.60	25.78	42.84	48.15	42.82
		100	21.60	24.82	18.27	32.26	36.15	31.49
		200	13.33	16.68	12.58	27.04	30.94	26.02
		300	13.52	16.86	12.79	24.27	27.85	23.46
	Ufal-Whisper [23]	40	48.95	60.24	49.75	57.40	71.35	55.83
		100	24.01	29.26	21.43	32.37	38.63	29.43
		200	12.14	14.18	11.04	20.57	22.64	**18.74**
		300	**8.21**	9.56	**7.60**	**16.78**	18.06	15.45
	CarelessWhisper	40	**11.11**	**14.85**	12.11	**23.61**	**25.90**	23.77
		100	**11.75**	**11.96**	10.63	**23.35**	**22.75**	**21.59**
		200	**10.19**	**10.08**	9.58	**20.44**	**19.80**	19.25
		300	9.36	**9.10**	9.04	19.15	18.37	18.03
	Offline Whisper [29]	-	-	-	5.00	-	-	12.40
small	Simul-Whisper [41]	40	17.07	21.52	14.68	29.17	35.64	32.71
		100	10.06	14.25	8.97	21.05	27.27	21.99
		200	8.03	13.22	7.58	18.02	23.41	19.26
		300	6.88	12.21	6.43	15.69	21.66	15.76
	Ufal-Whisper [23]	40	50.20	62.01	47.95	59.90	75.70	57.07
		100	19.57	27.02	17.99	27.26	35.01	24.50
		200	8.04	11.87	7.80	14.57	18.01	**13.45**
		300	**5.68**	7.40	**5.42**	**11.26**	**13.06**	**10.60**
	CarelessWhisper	40	**9.38**	**9.97**	**8.21**	**20.20**	**20.13**	**17.85**
		100	**8.88**	**8.82**	**7.69**	**18.00**	**17.28**	**16.15**
		200	**7.80**	**7.35**	**6.91**	16.03	**15.11**	14.62
		300	7.25	**6.93**	6.35	15.07	14.03	13.65
	Offline Whisper [29]	-	-	-	3.40	-	-	7.60
large-v2	Simul-Whisper [41]	40	14.59	17.05	13.63	26.07	28.44	24.62
		100	9.33	11.66	7.87	18.26	20.48	15.97
		200	6.62	9.19	5.61	14.65	17.30	13.24
		300	5.67	8.17	**4.57**	12.68	15.48	11.21
	Ufal-Whisper [23]	40	76.72	99.86	78.40	90.68	124.68	97.93
		100	32.15	40.50	27.64	40.57	49.94	35.27
		200	12.78	21.29	11.26	18.00	25.17	15.70
		300	6.79	16.82	7.50	**10.88**	18.82	10.76
	CarelessWhisper	40	**8.48**	**9.94**	**7.76**	**18.85**	**19.28**	**16.73**
		100	**6.38**	**7.76**	**6.33**	**14.31**	**14.99**	**13.06**
		200	**5.33**	**6.63**	5.92	**11.96**	**12.60**	**11.41**
		300	**4.72**	**6.00**	5.29	11.16	**11.38**	**10.74**
	Offline Whisper [29]	-	-	-	2.70	-	-	5.20

TABLE I: Performance across models, latency, and metrics. Best results per latency and dataset for each metric are in **bold**. Whisper results on a non streaming case are added for comparison.

Model	French			German			Portuguese			Spanish		
	RWER	ARWER	WER	RWER	ARWER	WER	RWER	ARWER	WER	RWER	ARWER	WER
Simul-Whisper [41]	17.4	20.65	15.24	16.20	24.79	20.40	18.44	22.15	17.16	11.58	16.03	11.64
Ufal-Whisper [23]	16.79	**15.94**	**12.40**	**13.83**	**15.21**	**11.40**	**14.39**	**14.26**	**11.85**	13.01	**12.85**	**9.98**
CarelessWhisper	**14.14**	17.24	14.23	14.07	17.54	14.45	18.26	20.19	16.49	**10.62**	13.63	10.55

TABLE II: WER Variants Across Languages, evaluated on *large-v2* models, using a chunk size of 300 msec, and an initial chunk size of 600 msec. Best results marked in **bold**.

enough linguistic diversity to generalize effectively across multiple languages.

4) Running with decoder self-attention KV-cache: CarelessWhisper enables the use of decoder self-attention KV-caching under certain assumptions. To assess the impact of KV-cache on transcription quality, we conducted an evaluation on the LibriSpeech *test-clean* set, using both greedy streaming decoding and beam search streaming decoding with beam sizes $b \in \{3, 5, 7\}$ and $n = 2$.

As shown in Figure 5, employing KV-cache in the decoder self-attention leads to a significant degradation in transcription performance. Although the encoder output is causal, the cross-attention mechanism appears to benefit from access to newly arriving frames, likely improving token prediction. This aligns with prior findings that not all attention heads function purely as alignment heads.

Without KV-cache, greedy decoding proves overly rigid, while larger beam sizes (e.g., $b = 7$) introduce degradation—possibly due to insufficient training data leading to poor distribution generalization. The best performance is achieved with a beam size of $b = 5$. Additionally, since input buffers may truncate words mid-utterance, hallucinations can occur, despite the model being fine-tuned to treat such events as stop conditions. When KV-cache is used, increasing the beam size
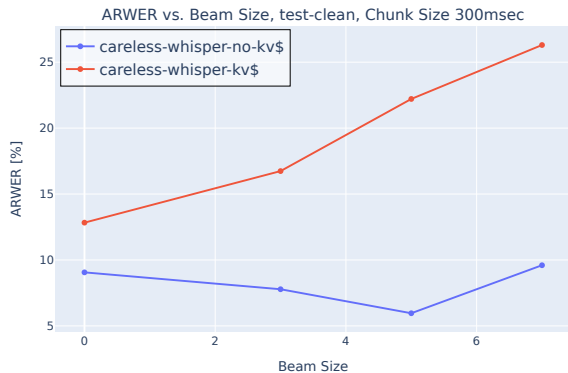
Fig. 5: ARWER vs. beam size on our method when using *large-v2* model. Decoder KV-cache models WER diverges quickly as beam size increases.
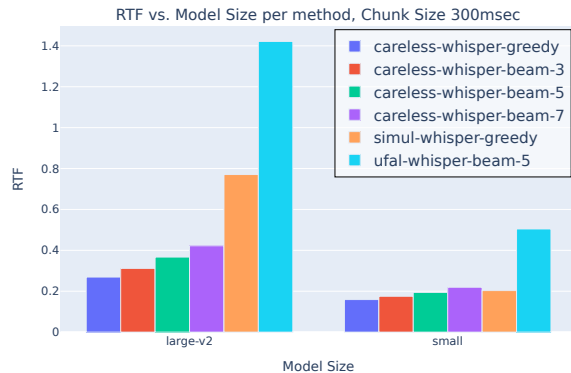

Fig. 6: RTF comparison on 300 msec chunk size streaming case simulation. Note that *Ufal-Whisper* runs faster whisper under the hood, using beam with size 5. *Simul-Whisper* uses greedy decoding.

leads to further performance decline. This suggests that once a token is emitted, it is unreasonable to assume its relevance to new acoustic inputs becomes negligible. Moreover, larger beam sizes exacerbate the effect of KV-caching, as the model cannot correct for the drift introduced by this assumption.

Future work may address this limitation by introducing regularization mechanisms to reduce the influence of non-alignment heads in cross-attention. Alternatively, a causal design of attention heads could be explored, encouraging stronger alignment between attention and acoustic input.

B. Runtime

We compared the runtime performance of our method against *Simul-Whisper* and *Ufal-Whisper*. During all experiments, we measured the latency per frame to compute both the average latency and the Real-Time Factor (RTF). All evaluations were performed on the LibriSpeech *test-clean* set using a DGX system equipped with $8\times$ NVIDIA A100 GPUs, each with 80GB of VRAM. To assess runtime efficiency, we used RTF, a common metric for streaming systems. For a given frame that requires t_c seconds to process and represents C seconds of audio, the RTF is defined as:

$$\text{RTF} = \frac{t_c}{C} \tag{27}$$

We report the mean RTF across all frames in the stream. Additionally, we report the average per-frame latency, i.e., the average processing time between receiving a new frame and completing its sinference.

Model	Beam Size	Avg. Latency (s) $\downarrow$
Ufal-Whisper [23]	5	0.426
Simul-Whisper [41]	0	0.231
CarelessWhisper	0	0.081
CarelessWhisper	3	0.094
CarelessWhisper	5	0.110
CarelessWhisper	7	0.127

TABLE III: Average latency for different models and beam sizes. All models are of size *large-v2* using a chunk size of 300 msec

As shown in Figure 6, our method consistently achieves faster inference times for both the *small* and *large-v2* model sizes. For the *large-v2* model, our method is nearly four times faster than *Ufal-Whisper* (comparing the same beam size, $b = 5$), and nearly three times faster than *Simul-Whisper*. For the *small* model, although the performance gap is smaller, our method still outperforms both baselines.

Notably, *Simul-Whisper* relies solely on greedy decoding, while *Ufal-Whisper* employs beam search with $b = 5$ and runs on the Fast Whisper backend. In contrast, our method uses the original OpenAI Whisper implementation, without any optimizations such as FlashAttention [5]. None of the compared methods implement decoder-side KV caching. Despite this, our approach remains faster—even when running our proposed streaming beam search with various beam sizes.

Importantly, the benefit of encoder-side KV caching becomes more pronounced with smaller chunk sizes, where the encoder's computational burden increases. Table III reports the average per-frame latency for our CarelessWhisper *large-v2* model with a chunk size of 300 msec. The empirical results align with the complexity analysis in Theorem 4. Unlike our method, both *Simul-Whisper* and *Ufal-Whisper* recompute full non-causal encoder self-attention at each step, adding substantial computational overhead. *Ufal-Whisper* incurs particularly high latency and RTF due to its local agreement mechanism, which is computationally expensive. While *Simul-Whisper*'s lightweight

cross-attention heuristic yields RTF values closer to ours for *s*mall models, the non-causal dot product operations result in significantly higher latency for larger models.

C. Word Level Timestamps

Our model was fine-tuned on weakly aligned data using a forced alignment algorithm [24], with a specific focus on learning when to stop emitting tokens and produce an end-of-transcription marker. This training strategy encourages the model to become more acoustically aligned, implicitly learning improved token boundary prediction. To assess the quality of the generated timestamps, we evaluated on the TIMIT [6] test dataset using *CarelessWhisper large-v2* models fine-tuned solely on English data, with chunk sizes of 40 msec and 100 msec.

Unlike forced-aligners, which receive the transcription as an input, our model functions as a standard ASR system that produces word-level timestamps as part of its transcription process. We report precision, recall, standard deviation (SD), and endpoint deviation (ED) metrics as defined in [14]. We evaluated our model against *NVIDIA Canary-180m-flash* and *NVIDIA Canary-1b-flash* models on the same test set. We chose the *NVIDIA Canary* family for comparison since its models naively generate word-level timestamps without relying on post-processing steps such as dynamic time warping [31], [32], which are commonly used in Whisper-based approaches [29].

Model	Metric Precision [%] ↑	Recall [%] ↑
CarelessWhisper small-40	88.6	82.8
CarelessWhisper large-v2-40	87.6	83.8
CarelessWhisper small-100	91.6	84.3
CarelessWhisper large-v2-100	91.7	86.8
NVIDIA Canary-180M-flash [14]	96.4	93.7
NVIDIA Canary-1B-flash [14]	**96.6**	**95.9**

TABLE IV: Comparison of our model against NVIDIA Canary models, using a threshold of 240 msec. The best results are **bold**. Our method presents two different sizes, and two different chunk sizes (40 msec, and 100 msec).

Using a threshold of 240 msec, both *Canary* models achieve higher precision and recall, as shown in Table IV. However, they under-perform in terms of Start Difference (SD) and End Difference (ED), as presented in Table V. Our method, particularly when using the smallest chunk size, yields better performance with respect to start and end boundary accuracy on the TIMIT test set.

Model	Metric SD [msec] ↓	ED [msec] ↓
CarelessWhisper small-40	71.6	**67.3**
CarelessWhisper large-v2-40	**70.7**	75.8
CarelessWhisper small-100	74.7	81.0
CarelessWhisper large-v2-100	73.1	81.8
NVIDIA Canary-180m-flash [14]	82.6	71.3
NVIDIA canary-1b-flash [14]	74.5	71.6

TABLE V: Comparison of our model against NVIDIA Canary models. The best results are **bold**. Our method presents two different sizes. Our method achieves best SD ED values when using models that were fine-tuned with chunk size of 40 msec

When reducing the threshold from 240 msec to 80 msec, as shown in Table VI, the precision of both *Canary* models drops significantly. In contrast, both of our models maintain higher precision, indicating improved word-level timestamp resolution compared to *Canary* models, though at the cost of transcription accuracy. It is important to note that *Canary* models are not designed for streaming, and given the definitions of precision and recall in [14], models with better transcription accuracy are naturally favored by these metrics. The evaluation excludes words that ended within the first 600 msec – the initial chunk size used by all our models. Additionally, despite relying on the assumption that the beginning of a current word aligns with the end of the previous one, our models achieve better average timestamp accuracy than the *Canary* models.

Model	Metric Precision [%] ↑	Recall [%] ↑
CarelessWhisper small-40	64.4	77.8
CarelessWhisper large-v2-40	**64.8**	79.4
CarelessWhisper small-100	56.1	76.8
CarelessWhisper large-v2-100	56.8	80.3
NVIDIA Canary-180m-flash [14]	38.5	85.6
NVIDIA Canary-1b-flash [14]	42.3	**91.1**

TABLE VI: Comparison of our model against NVIDIA Canary models , using a threshold of 80 msec. The best results are **bold**. Our method presents two different sizes, and two different chunk sizes (40 msec, and 100 msec).

VIII. CONCLUSION, DISCUSSION, FUTURE WORK

We proposed a method for adapting a non-causal transformer ASR model, such as Whisper, into a causal variant that enables significantly faster real-time transcription with minimal performance degradation and reduced computational cost per transcription. An additional benefit of our training approach is the model's ability to produce word-level timestamps using a simple and naive decoding strategy. Leveraging LoRA, our approach supports a dual-setup model that can be dynamically switched based on user requirements, with negligible memory overhead. We also presented a runtime complexity analysis of the proposed method. The main limitation of our approach is the need to train a separate model for each chunk size. A potential direction for future work is to introduce randomization in the masking scheme. Furthermore, the method does not yet address the limitations associated with using a decoder KV-cache in streaming scenarios. One possible solution is to mask the cross-attention heads to enforce alignment with the input acoustics, rather than relying on sparsity assumptions in regions temporally distant from the token's origin.

REFERENCES

[1] Alexei Baevski, Henry Zhou, Abdelrahman Mohamed, and Michael Auli. wav2vec 2.0: A framework for self-supervised learning of speech representations, 2020.

[2] Peikun Chen, Sining Sun, Changhao Shan, Qing Yang, and Lei Xie. Streaming decoder-only automatic speech recognition with discrete speech units: A pilot study, 2024.

[3] Xie Chen, Yu Wu, Zhenghao Wang, Shujie Liu, and Jinyu Li. Developing real-time streaming transformer transducer for speech recognition on large-scale dataset. In *ICASSP 2021-2021 IEEE International Conference on Acoustics, Speech and Signal Processing (ICASSP)*, pages 5904–5908. IEEE, 2021.

[4] Kwanghee Choi, Masao Someki, Emma Strubell, and Shinji Watanabe. On-device streaming discrete speech units. *arXiv preprint arXiv:2506.01845*, 2025.

[5] Tri Dao, Daniel Y. Fu, Stefano Ermon, Atri Rudra, and Christopher Ré. Flashattention: Fast and memory-efficient exact attention with io-awareness, 2022.

[6] John S. Garofolo, Lori F. Lamel, William M. Fisher, Jonathan G. Fiscus, David S. Pallett, and Nancy L. Dahlgren. TIMIT acoustic-phonetic continuous speech corpus, 1993. LDC93S1.

[7] Alex Graves. Sequence transduction with recurrent neural networks, 2012.

[8] Alex Graves, Santiago Fernández, Faustino Gomez, and Jürgen Schmidhuber. Connectionist temporal classification: labelling unsegmented sequence data with recurrent neural networks. In *Proceedings of the 23rd international conference on Machine learning*, pages 369–376, 2006.

[9] Yanzhang He, Tara N Sainath, Rohit Prabhavalkar, Ian McGraw, Raziel Alvarez, Ding Zhao, David Rybach, Anjuli Kannan, Yonghui Wu, Ruoming Pang, et al. Streaming end-to-end speech recognition for mobile devices. In *ICASSP 2019-2019 IEEE International Conference on Acoustics, Speech and Signal Processing (ICASSP)*, pages 6381–6385. IEEE, 2019.

[10] Geoffrey Hinton, Oriol Vinyals, and Jeff Dean. Distilling the knowledge in a neural network. *arXiv preprint arXiv:1503.02531*, 2015.

[11] Sepp Hochreiter and Jürgen Schmidhuber. Long short-term memory. *Neural computation*, 9(8):1735–1780, 1997.

[12] Wei-Ning Hsu, Benjamin Bolte, Yao-Hung Hubert Tsai, Kushal Lakhotia, Ruslan Salakhutdinov, and Abdelrahman Mohamed. Hubert: Self-supervised speech representation learning by masked prediction of hidden units, 2021.

[13] Edward J. Hu, Yelong Shen, Phillip Wallis, Zeyuan Allen-Zhu, Yuanzhi Li, Shean Wang, Lu Wang, and Weizhu Chen. Lora: Low-rank adaptation of large language models, 2021.

[14] Ke Hu, Krishna Puvvada, Elena Rastorgueva, Zhehuai Chen, He Huang, Shuoyang Ding, Kunal Dhawan, Hainan Xu, Jagadeesh Balam, and Boris Ginsburg. Word level timestamp generation for automatic speech recognition and translation, 2025.

[15] Junteng Jia, Gil Keren, Wei Zhou, Egor Lakomkin, Xiaohui Zhang, Chunyang Wu, Frank Seide, Jay Mahadeokar, and Ozlem Kalinli. Efficient streaming llm for speech recognition. *arXiv preprint arXiv:2410.03752*, 2024.

[16] Shashi Kumar, Srikanth Madikeri, Juan Zuluaga-Gomez, Esaú Villatoro-Tello, Iuliia Thorbecke, Petr Motlicek, Manjunath K E, and Aravind Ganapathiraju. Xlsr-transducer: Streaming asr for self-supervised pretrained models, 2024.

[17] Gakuto Kurata and George Saon. Knowledge distillation from offline to streaming rnn transducer for end-to-end speech recognition. In *Interspeech*, pages 2117–2121, 2020.

[18] Jinyu Li, Rui Zhao, Jui-Ting Huang, and Yifan Gong. Learning small-size dnn with output-distribution-based criteria. In *interspeech*, pages 1910–1914, 2014.

[19] Shen Li, Yanli Zhao, Rohan Varma, Omkar Salpekar, Pieter Noordhuis, Teng Li, Adam Paszke, Jeff Smith, Brian Vaughan, Pritam Damania, and Soumith Chintala. Pytorch distributed: Experiences on accelerating data parallel training, 2020.

[20] Danni Liu, Gerasimos Spanakis, and Jan Niehues. Low-latency sequence-to-sequence speech recognition and translation by partial hypothesis selection. *arXiv preprint arXiv:2005.11185*, 2020.

[21] Ilya Loshchilov and Frank Hutter. Decoupled weight decay regularization, 2019.

[22] Liang Lu, Michelle Guo, and Steve Renals. Knowledge distillation for small-footprint highway networks. In *2017 IEEE International Conference on Acoustics, Speech and Signal Processing (ICASSP)*, pages 4820–4824. IEEE, 2017.

[23] Dominik Macháček, Raj Dabre, and Ondřej Bojar. Turning whisper into real-time transcription system. *arXiv preprint arXiv:2307.14743*, 2023.

[24] Michael McAuliffe, Michaela Socolof, Sarah Mihuc, Michael Wagner, and Morgan Sonderegger. Montreal forced aligner: Trainable text-speech alignment using kaldi. In *Interspeech*, volume 2017, pages 498–502, 2017.

[25] Niko Moritz, Takaaki Hori, and Jonathan Le. Streaming automatic speech recognition with the transformer model. In *ICASSP 2020-2020 IEEE International Conference on Acoustics, Speech and Signal Processing (ICASSP)*, pages 6074–6078. IEEE, 2020.

[26] Niko Moritz, Takaaki Hori, and Jonathan Le Roux. Triggered attention for end-to-end speech recognition. In *ICASSP 2019-2019 IEEE International Conference on Acoustics, Speech and Signal Processing (ICASSP)*, pages 5666–5670. IEEE, 2019.

[27] Niko Moritz, Takaaki Hori, and Jonathan Le Roux. Dual causal/non-causal self-attention for streaming end-to-end speech recognition. *arXiv preprint arXiv:2107.01269*, 2021.

[28] Vassil Panayotov, Guoguo Chen, Daniel Povey, and Sanjeev Khudanpur. Librispeech: an asr corpus based on public domain audio books. In *2015 IEEE international conference on acoustics, speech and signal processing (ICASSP)*, pages 5206–5210. IEEE, 2015.

[29] Alec Radford, Jong Wook Kim, Tao Xu, Greg Brockman, Christine McLeavey, and Ilya Sutskever. Robust speech recognition via large-scale weak supervision, 2022.

[30] Kanishka Rao, Haşim Sak, and Rohit Prabhavalkar. Exploring architectures, data and units for streaming end-to-end speech recognition with rnn-transducer. In *2017 IEEE automatic speech recognition and understanding workshop (ASRU)*, pages 193–199. IEEE, 2017.

[31] Hiroaki Sakoe. Dynamic-programming approach to continuous speech recognition. In *1971 Proc. the International Congress of Acoustics, Budapest*, 1971.

[32] Hiroaki Sakoe and Seibi Chiba. Dynamic programming algorithm optimization for spoken word recognition. *IEEE transactions on acoustics, speech, and signal processing*, 26(1):43–49, 2003.

[33] Steffen Schneider, Alexei Baevski, Ronan Collobert, and Michael Auli. wav2vec: Unsupervised pre-training for speech recognition, 2019.

[34] Mike Schuster and Kuldip K Paliwal. Bidirectional recurrent neural networks. *IEEE transactions on Signal Processing*, 45(11):2673–2681, 1997.

[35] Yangyang Shi, Yongqiang Wang, Chunyang Wu, Ching-Feng Yeh, Julian Chan, Frank Zhang, Duc Le, and Mike Seltzer. Emformer: Efficient memory transformer based acoustic model for low latency streaming speech recognition. In *ICASSP 2021-2021 IEEE International Conference on Acoustics, Speech and Signal Processing (ICASSP)*, pages 6783–6787. IEEE, 2021.

[36] Anshuman Tripathi, Jaeyoung Kim, Qian Zhang, Han Lu, and Hasim Sak. Transformer transducer: One model unifying streaming and non-streaming speech recognition. *arXiv preprint arXiv:2010.03192*, 2020.

[37] Emiru Tsunoo, Hayato Futami, Yosuke Kashiwagi, Siddhant Arora, and Shinji Watanabe. Decoder-only architecture for streaming end-to-end speech recognition, 2024.

[38] Emiru Tsunoo, Yosuke Kashiwagi, and Shinji Watanabe. Streaming transformer asr with blockwise synchronous beam search. In *2021 IEEE Spoken Language Technology Workshop (SLT)*, pages 22–29. IEEE, 2021.

[39] Ashish Vaswani, Noam Shazeer, Niki Parmar, Jakob Uszkoreit, Llion Jones, Aidan N. Gomez, Lukasz Kaiser, and Illia Polosukhin. Attention is all you need, 2023.

[40] Chengyi Wang, Yu Wu, Shujie Liu, Jinyu Li, Liang Lu, Guoli Ye, and Ming Zhou. Low latency end-to-end streaming speech recognition with a scout network. *arXiv preprint arXiv:2003.10369*, 2020.

[41] Haoyu Wang, Guoqiang Hu, Guodong Lin, Wei-Qiang Zhang, and Jian Li. Simul-whisper: Attention-guided streaming whisper with truncation detection. *arXiv preprint arXiv:2406.10052*, 2024.

[42] Rongxiang Wang, Zhiming Xu, and Felix Xiaozhu Lin. Efficient whisper on streaming speech. *arXiv preprint arXiv:2412.11272*, 2024.

[43] Chunyang Wu, Yongqiang Wang, Yangyang Shi, Ching-Feng Yeh, and Frank Zhang. Streaming transformer-based acoustic models using self-attention with augmented memory. *arXiv preprint arXiv:2005.08042*, 2020.

[44] Ching-Feng Yeh, Jay Mahadeokar, Kaustubh Kalgaonkar, Yongqiang Wang, Duc Le, Mahaveer Jain, Kjell Schubert, Christian Fuegen, and Michael L Seltzer. Transformer-transducer: End-to-end speech recognition with self-attention. *arXiv preprint arXiv:1910.12977*, 2019.

[45] Qian Zhang, Han Lu, Hasim Sak, Anshuman Tripathi, Erik McDermott, Stephen Koo, and Shankar Kumar. Transformer transducer: A streamable speech recognition model with transformer encoders and rnn-t loss. In *ICASSP 2020-2020 IEEE International Conference on Acoustics, Speech and Signal Processing (ICASSP)*, pages 7829–7833. IEEE, 2020.

[46] Haoran Zhou, Xingchen Song, Brendan Fahy, Qiaochu Song, Binbin Zhang, Zhendong Peng, Anshul Wadhawan, Denglin Jiang, Apurv Verma, Vinay Ramesh, Srivas Prasad, and Michele M. Franceschini. Adapting whisper for streaming speech recognition via two-pass decoding, 2025.

APPENDIX A
THEOREMS PROOFS

Theorem 1. *Let $k\tau < T$, where k is the frame index and τ is the chunk size. Denote by $\mathbf{X}_T$, and by $\mathbf{X}_{k\tau}$ the full and*

the truncated inputs to the encoder, respectively. Let $\mathbf{Z}_T =$ Encoder($\mathbf{X}_T$) *and let* $\mathbf{Z}_{k\tau} =$ Encoder($\mathbf{X}_{k\tau}$). *Then*

$$[\mathbf{Z}_T]_t \neq [\mathbf{Z}_{k\tau}]_t \quad 1 \leq t \leq k\tau , \qquad (28)$$

where $[\mathbf{Z}_T]_t$ *is the* t*-th representation.*

Proof of Theorem 1. Let $\mathbf{Q}_{k\tau}, \mathbf{K}_{k\tau}, \mathbf{V}_{k\tau}$ be the queries, values of $\mathbf{U}_{k\tau}$, and similarly let $\mathbf{Q}_T, \mathbf{K}_T, \mathbf{V}_T$ be the queries, keys and values of $\mathbf{U}_T$. By definition:

$$\text{SA}(\mathbf{U}_{k\tau}) = \text{Softmax}\left(\frac{\mathbf{Q}_{k\tau}\mathbf{K}_{k\tau}^\top}{\sqrt{d}}\right)\mathbf{V}_{k\tau} \qquad (29)$$

$$\text{SA}(\mathbf{U}_T) = \text{Softmax}\left(\frac{\mathbf{Q}_T\mathbf{K}_T^\top}{\sqrt{d}}\right)\mathbf{V}_T \qquad (30)$$

Let us inspect the t-th ($t \leq k\tau < T$) row of the results:

$$\text{SA}(\mathbf{U}_{k\tau})_t = \frac{\sum_{j=1}^{k\tau} \exp\left(\frac{[\mathbf{Q}_{k\tau}]_t^\top \cdot [\mathbf{K}_{k\tau}]_j}{\sqrt{d}}\right) \cdot [\mathbf{V}_{k\tau}]_j}{\sum_{j=1}^{k\tau} \exp\left(\frac{[\mathbf{Q}_{k\tau}]_t^\top \cdot [\mathbf{K}_{k\tau}]_j}{\sqrt{d}}\right)} \qquad (31)$$

$$\text{SA}(\mathbf{U}_T)_t = \frac{\sum_{j=1}^{T} \exp\left(\frac{[\mathbf{Q}_T]_t^\top \cdot [\mathbf{K}_T]_j}{\sqrt{d}}\right) \cdot [\mathbf{V}_T]_j}{\sum_{j=1}^{T} \exp\left(\frac{[\mathbf{Q}_T]_t^\top \cdot [\mathbf{K}_T]_j}{\sqrt{d}}\right)} \qquad (32)$$

$$\qquad (33)$$

And since $k\tau < T$:

$$\text{SA}(\mathbf{U}_{k\tau})_t \neq \text{SA}(\mathbf{U}_T)_t \qquad (34)$$

Since the encoder function can be described as:

$$\text{Encoder}(\mathbf{X}) = f\left(\mathbf{W}(\text{SA}(\mathbf{X}) + \mathbf{X}) + \mathbf{b}\right) \qquad (35)$$

Since the SA arguments and outputs are not equal, we can conclude that:

$$[\mathbf{Z}_{k\tau}]_t \neq [\mathbf{Z}_T]_t \quad \forall 1 \leq t \leq k\tau \qquad (36)$$

$\square$

We emphasize the importance of fine-tuning the model in order for it to be able represent data causally. To do so, we observe the difference of the i-th encoder self-attention output vector, when given k chunks, and when given $k+1$ chunks.

$$\left\|\Delta(\mathbf{U}_{k\tau}, \mathbf{U}_{(k+1)\tau})_i\right\|_2 \triangleq \left\|\text{SA}(\mathbf{U}_{k\tau})_i - \text{SA}(\mathbf{U}_{(k+1)\tau})_i\right\|_2 \qquad (37)$$

From self-attention definition we get an upper bound on the difference, when assuming $\|\mathbf{V}_n\|_2 < \epsilon, \forall n, \epsilon > 0$ (i.e., all value vectors norms are bounded by a constant $\epsilon > 0$) as can be seen by Eq. (61). It is clear that $\left\|\Delta(\mathbf{U}_{k\tau}, \mathbf{U}_{(k+1)\tau})_i\right\|_2 \neq 0$ as long as $[\mathbf{Q}_{k\tau}]_i^\top[\mathbf{K}_{k\tau}]_j \neq -\infty$. Thus, any future data that is added during the streaming process, adds a delta that is not null to a previous encoder outputs. This behavior leads us to use a causal masking approach on the encoder self-attention weights, since our motivation is not to re-calculate past encoder representations, due to inefficiency.

A concrete formula for constructing the mask given the parameters, τ, τ_0 is available on (38).

$$\mathbf{M}_{ij}(k, \tau, \tau_0) = \begin{cases} 0 & \lceil\frac{i}{\tau}\rceil \geq \lceil\frac{j}{\tau}\rceil \vee (i,j) \in [1, \tau_0] \times [1, \tau_0] \\ -\infty & \text{otherwise} \end{cases} \qquad (38)$$

Theorem 2. *Let* $k\tau < T$, *where* k *is the chunk index and* τ *is the chunk size. Denote by* $\mathbf{X}_T$, *and by* $\mathbf{X}_{k\tau}$ *the full and the truncated inputs to the encoder respectively. Let* $\tilde{\mathbf{Z}}_T = $ StreamingEncoder($\mathbf{X}_T$) *and let* $\tilde{\mathbf{Z}}_{k\tau} = $ StreamingEncoder($\mathbf{X}_{k\tau}$). *Then*

$$[\tilde{\mathbf{Z}}_T]_t = [\tilde{\mathbf{Z}}_{k\tau}]_t \quad 1 \leq t \leq k\tau \qquad (39)$$

where $[\tilde{\mathbf{Z}}_T]_t$ *is the* t*-th representation.*

Proof of Theorem 2. Let $\mathbf{Q}_{k\tau}, \mathbf{K}_{k\tau}, \mathbf{V}_{k\tau}$ be the queries, values of $\mathbf{U}_\tau$, and similarly let $\mathbf{Q}_T, \mathbf{K}_T, \mathbf{V}_T$ be the queries, keys and values of $\mathbf{U}_T$. Let us inspect the t-th ($t \leq k\tau < T$) row of the results:

$$\widetilde{\text{SA}}(\mathbf{U}_{k\tau})_t = \frac{\sum_{j=1}^{k\tau} \exp\left(\frac{[\mathbf{Q}_{k\tau}]_t^\top \cdot [\mathbf{K}_{k\tau}]_j + \mathbf{M}_{tj}}{\sqrt{d}}\right) \cdot [\mathbf{V}_{k\tau}]_j}{\sum_{j=1}^{k\tau} \exp\left(\frac{[\mathbf{Q}_{k\tau}]_t^\top \cdot [\mathbf{K}_{k\tau}]_j + \mathbf{M}_{tj}}{\sqrt{d}}\right)} \qquad (40)$$

$$\widetilde{\text{SA}}(\mathbf{U}_T)_t = \frac{\sum_{j=1}^{T} \exp\left(\frac{[\mathbf{Q}_T]_t^\top \cdot [\mathbf{K}_T]_j + M_{tj}}{\sqrt{d}}\right) \cdot [\mathbf{V}_T]_j}{\sum_{j=1}^{T} \exp\left(\frac{[\mathbf{Q}_T]_t^\top \cdot [\mathbf{K}_T]_j + M_{tj}}{\sqrt{d}}\right)} \qquad (41)$$

From the mask construction:

$$\widetilde{\text{SA}}(\mathbf{U}_{k\tau})_t = \frac{\sum_{j=1}^{\lceil\frac{t}{m}\rceil} \exp\left(\frac{[\mathbf{Q}_{k\tau}]_t^\top \cdot [\mathbf{K}_{k\tau}]_j}{\sqrt{d}}\right) \cdot [\mathbf{V}_{k\tau}]_j}{\sum_{j=1}^{\lceil\frac{t}{m}\rceil} \exp\left(\frac{[\mathbf{Q}_{k\tau}]_t^\top \cdot [\mathbf{K}_{k\tau}]_j}{\sqrt{d}}\right)} \qquad (42)$$

$$\widetilde{\text{SA}}(\mathbf{U}_T)_t = \frac{\sum_{j=1}^{\lceil\frac{t}{m}\rceil} \exp\left(\frac{[\mathbf{Q}_T]_t^\top \cdot [\mathbf{K}_T]_j}{\sqrt{d}}\right) \cdot [\mathbf{V}_T]_j}{\sum_{j=1}^{\lceil\frac{t}{m}\rceil} \exp\left(\frac{[\mathbf{Q}_T]_t^\top \cdot [\mathbf{K}_T]_j}{\sqrt{d}}\right)} \qquad (43)$$

Since $\mathbf{X}_{k\tau} = [\mathbf{X}_T]_1^{k\tau}$:

$$[\mathbf{Q}_{k\tau}]_t = [\mathbf{Q}_T]_t, [\mathbf{K}_{k\tau}]_1^{\lceil\frac{t}{m}\rceil} = [\mathbf{K}_T]_1^{\lceil\frac{t}{m}\rceil}, [\mathbf{V}_{k\tau}]_1^{\lceil\frac{t}{m}\rceil} = [\mathbf{V}_T]_1^{\lceil\frac{t}{m}\rceil} \qquad (44)$$

Therefore:

$$\widetilde{\text{SA}}(\mathbf{U}_{k\tau})_t = \widetilde{\text{SA}}(\mathbf{U}_T)_t \quad \forall t \leq k\tau \qquad (45)$$

Since the encoder function can be described as:

$$\text{StreamingEncoder}(\mathbf{U}) = f\left(\mathbf{W}(\widetilde{\text{SA}}(\mathbf{U}) + \mathbf{U}) + \mathbf{b}\right) \qquad (46)$$

And the $\widetilde{\text{SA}}$ arguments and outputs are equal, we can conclude that:

$$[\tilde{\mathbf{Z}}_{k\tau}]_t = [\tilde{\mathbf{Z}}_T]_t \quad \forall t \leq k\tau \qquad (47)$$

$\square$

Theorem 3 (Streaming Greedy Decoding Optimality). *Let*

$$P^*(y_i \mid \mathbf{y}_{<i}, \mathbf{X}_{k\tau}) \qquad (48)$$

be the optimal probability distribution of the i*-th token given the preceding tokens, and the acoustic data till* $k\tau$. *Denote by* ρ_k *the probability path of the predicted token sequence until the chunk* k. *Our proposed greedy decoding algorithm, as depicted on Algo. 4, is optimal in the sense that it yields a probability path* ρ_k^{CW} *which is larger or equal on the probability path of the greedy algorithm,* ρ_k^G.

Proof of Theorem 3. We prove the claim using mathematical induction. For the first chunk $k = 1$ both algorithms choose the same tokens hence have same probability path:

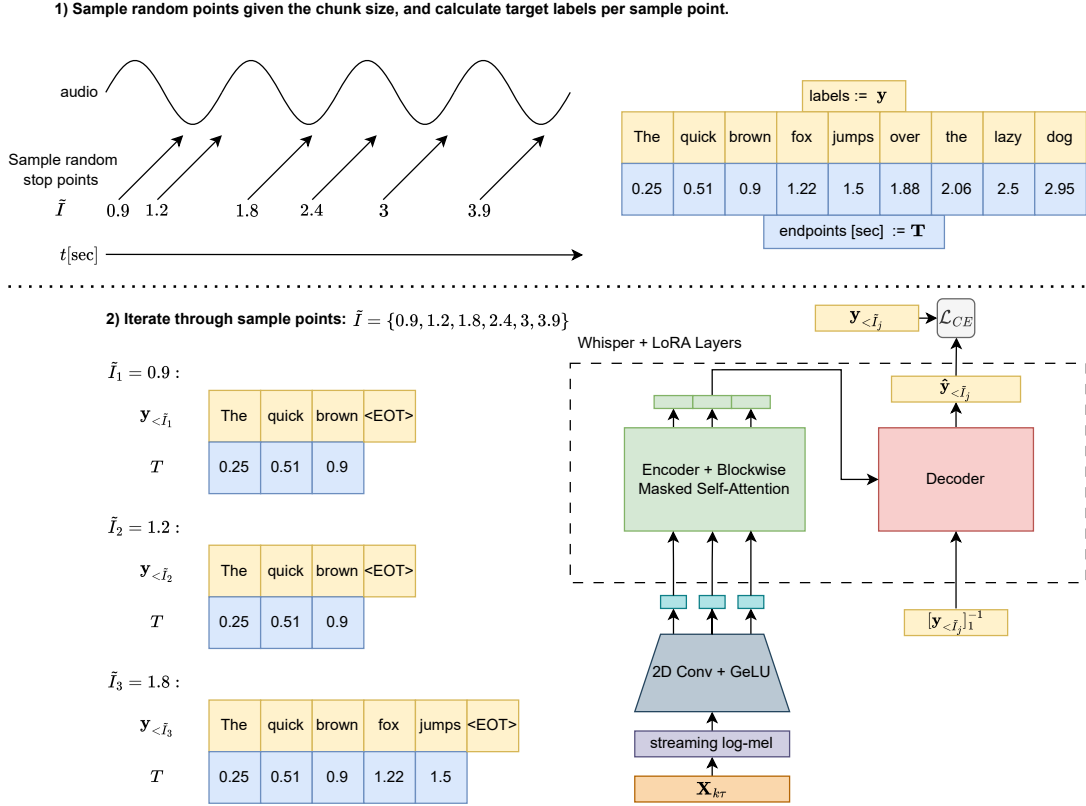$$\rho_1^{\text{CW}} \geq \rho_1^G \qquad (49)$$

Fig. 7: Fine-tuning process illustration. The above example demonstrates an encoder that uses a chunk size of size 300 msec. Using such method makes training more efficient, since there is no need to go through each possible frame in the streaming process.

Assuming the statement is correct for any k, we will prove that it holds for $k+1$. For the case of k, the greedy decoder continues its prediction from where it previously stopped. The algorithm needs to determine how to handle the token at index $i-m$ considering the options: 1) If $y_{i-m} = j$ is unstable, it means:

$$P(y_{i-m} = j \mid \mathbf{y}_{<i-m}, \mathbf{X}_{(k+1)\tau})$$
$$< \max_{v \in \mathcal{V}} P(y_{i-m} \mid \mathbf{y}_{<i-m}, \mathbf{X}_{(k+1)\tau}) \quad (50)$$

and

$$P(y_{i-m} = j \mid \mathbf{y}_{<i-m}, \mathbf{X}_{(k+1)\tau})$$
$$< P(y_{i-m} = j \mid \mathbf{y}_{<i-m}, \mathbf{X}_{k\tau}) \quad (51)$$

2) If $y_{i-m} = j$ is stable, either:

$$j = \arg\max_{u \in \mathcal{V}} P(y_{i-m} = u \mid \mathbf{y}_{<i-m}, \mathbf{X}_{k\tau}) . \quad (52)$$

or

$$P(y_{i-m} = j \mid \mathbf{y}_{<i-m}, \mathbf{X}_{k\tau}) \geq P(y_{i-m} = j \mid \mathbf{y}_{<i-m}, \mathbf{X}_{(k-1)\tau}) \quad (53)$$

holds. Either way, y_{i-m} token is a token with higher probability than the last frame. Thus, $\rho_{k+1}^{CW} \geq \rho_{k+1}^{G}$

$\square$

Theorem 4. *Let T be the input sequence length to the encoder, d the embedding dimension, and τ the chunk size, with $0 <$ $\tau \ll T$. The computation of blocked causal attention over the full sequence during streaming requires $\mathcal{O}(T^2 d + Td^2)$ operations and $\mathcal{O}(Td)$ additional memory.*

Proof of theorem 4. We break down the attention calculation process. We observe a process of an arbitrary chunk during the streaming process, let it be chunk i, $1 \leq i \leq \frac{T}{\tau}$. First, the encoder calculates the projections $\mathbf{Q}, \mathbf{K}, \mathbf{V} \in \mathbb{R}^{\tau \times d}$ of the received chunk. Such calculation requires $\mathcal{O}(\tau d^2)$ operations. In addition, an extra $\mathcal{O}(\tau d)$ memory is required to cache $\mathbf{K}, \mathbf{V}$ of the received chunk. For the dot product calculation, each chunk attends only to previous chunks. Thus, the i-th chunk, requires $\mathcal{O}(i\tau^2 d)$ operations to calculate the dot product results. In order to calculate the number of operations required to calculate the causal encoder output sequence of length T, we sum over the operations per chunk. For the projections calculation:

$$\sum_{i=1}^{\frac{T}{\tau}} \tau d^2 = \frac{T}{\tau} \cdot \tau d^2 = Td^2 \quad (54)$$

Overall, $\mathcal{O}(Td^2)$ operations required. When summing over the required operations for the dot products:

$$\sum_{i=1}^{\frac{T}{\tau}} i\tau^2 d = \frac{\tau^2 d}{2}\left(\frac{T^2}{\tau^2} + \frac{T}{\tau}\right) \quad (55)$$

$$= \frac{T^2}{2} \cdot d + \frac{T}{2} \cdot \tau d \quad (56)$$

Overall, $\mathcal{O}(T^2 d)$ operations required. For the memory complexity, we recall that $\mathcal{O}(\tau d)$ is the memory required per chunk, given $\frac{T}{\tau}$ chunks, we get $\mathcal{O}(Td)$ extra memory required. $\qquad\square$

APPENDIX B
DECODING WITH ONLINE TIMESTAMPS

Algorithm 4 Streaming Greedy Decoding with Word Level Timestamps

---

1: **Input:** n
2: **Output:** $\hat{\mathbf{y}}$, timestamps
3: $\hat{\mathbf{y}} \leftarrow \varnothing$
4: timestamps $\leftarrow \varnothing$
5: completed $\leftarrow \varnothing$
6: **for** $k \in \{0, \ldots, \frac{T}{\tau}\}$ **do**
7:    new_chunk $\leftarrow$ True
8:    **while** not completed **do**
9:      **if** new_chunk **then**
10:        new_chunk $\leftarrow$ False
       // Check for unstable tokens
11:        **for** $m \in \{n-1, n-2, \ldots, 0\}$ **do**
12:          **if** token y_{i-m} is unstable **then**
13:            $\hat{\mathbf{y}} \leftarrow \hat{\mathbf{y}}_{<i-m}$
14:            **break**
15:          **end if**
16:        **end for**
17:      **end if**
     // Decode greedily
18:      $\hat{\mathbf{y}} \leftarrow \hat{\mathbf{y}}_{<i-m} \oplus \arg\max\left(P(\hat{y}_{i-m}|\hat{\mathbf{y}}_{<i-m}, \mathbf{X}_{k\tau})\right)$
19:      completed $\leftarrow EOT \in \hat{\mathbf{y}}$
20:      **if** not completed and $m = 0$ **then**
21:        timestamps$_i \leftarrow k\tau$
22:      **end if**
23:    **end while**
24: **end for**
25: **return** $\hat{\mathbf{y}}$, timestamps

APPENDIX C
TRAINING DETAILS

A. English Transcription

We fine-tuned our model using 960 hours of Librispeech-train dataset. All of the models variants were trained with an initial learning rate of 1e-5, using an AdamW [21] optimizer, weight decay of 0.01 and a *ReduceLROnPlateau* learning rate scheduler with factor of 0.5 and patience of 2 epochs. The *base* and *small* variants were trained using batch size of 32 and 16 respectively. Both models were trained for 10 epochs. The *large-v2* models were trained using a batch size of 4 and for 3 epochs. Rest of the hyper parameters are detailed on Table VII. We used PyTorch Lightning framework to accelerate the training process, using DDP [19] strategy.

Model	Chunk Size (ms)	Rank	Extra Chunks	Points Fraction $\hat{f}$
Base	40	32	14	0.02
	100	32	5	0.05
	200	32	2	0.10
	300	32	1	0.25
Small	40	32	14	0.02
	100	32	5	0.05
	200	32	2	0.10
	300	32	1	0.25
	1000	32	0	0.40
Large-v2	40	4	14	0.02
	100	4	5	0.05
	200	4	2	0.07
	300	4	1	0.1
	1000	4	0	0.3

TABLE VII: Fine-tuning parameters for each model variant and chunk size

B. Multilingual Transcription

We fine-tuned a single *large-v2* model on a Multilingual LibriSpeech (MLS) corpus, excluding the english partition,

$$\left\|\Delta(\mathbf{U}_{k\tau}, \mathbf{U}_{(k+1)\tau})_i\right\|_2 = \left\|\frac{\sum_{j=1}^{(k+1)\tau} \exp\left(\frac{[\mathbf{Q}_{(k+1)\tau}]_i^\top [\mathbf{K}_{(k+1)\tau}]_j}{\sqrt{d}}\right) \cdot \mathbf{V}_j}{\sum_{j=1}^{(k+1)\tau} \exp\left(\frac{[\mathbf{Q}_{(k+1)\tau}]_i^\top [\mathbf{K}_{(k+1)\tau}]_j}{\sqrt{d}}\right)} - \frac{\sum_{j=1}^{k\tau} \exp\left(\frac{[\mathbf{Q}_{k\tau}]_i^\top [\mathbf{K}_{k\tau}]_j}{\sqrt{d}}\right) \cdot \mathbf{V}_j}{\sum_{j=1}^{k\tau} \exp\left(\frac{[\mathbf{Q}_{k\tau}]_i^\top [\mathbf{K}_{k\tau}]_j}{\sqrt{d}}\right)}\right\| \tag{57}$$

$$= \left\|\frac{\sum_{j=1}^{k\tau} \exp\left(\frac{[\mathbf{Q}_{k\tau}]_i^\top [\mathbf{K}_{k\tau}]_j}{\sqrt{d}}\right) \sum_{m=k\tau+1}^{(k+1)\tau} \exp\left(\frac{[\mathbf{Q}_{(k+1)\tau}]_i^\top [\mathbf{K}_{(k+1)\tau}]_m}{\sqrt{d}}\right) \cdot (\mathbf{V}_m - \mathbf{V}_j)}{\sum_{j=1}^{k\tau} \exp\left(\frac{[\mathbf{Q}_{k\tau}]_i^\top [\mathbf{K}_{k\tau}]_j}{\sqrt{d}}\right) \cdot \sum_{m=1}^{(k+1)\tau} \exp\left(\frac{[\mathbf{Q}_{(k+1)\tau}]_i^\top [\mathbf{K}_{(k+1)\tau}]_m}{\sqrt{d}}\right)}\right\| \tag{58}$$

$$\leq \frac{\sum_{j=1}^{k\tau} \exp\left(\frac{[\mathbf{Q}_{k\tau}]_i^\top [\mathbf{K}_{k\tau}]_j}{\sqrt{d}}\right) \sum_{m=k\tau+1}^{(k+1)\tau} \exp\left(\frac{[\mathbf{Q}_{(k+1)\tau}]_i^\top [\mathbf{K}_{(k+1)\tau}]_m}{\sqrt{d}}\right) \cdot \|\mathbf{V}_m - \mathbf{V}_j\|}{\sum_{j=1}^{k\tau} \exp\left(\frac{[\mathbf{Q}_{k\tau}]_i^\top [\mathbf{K}_{k\tau}]_j}{\sqrt{d}}\right) \cdot \sum_{m=1}^{(k+1)\tau} \exp\left(\frac{[\mathbf{Q}_{(k+1)\tau}]_i^\top [\mathbf{K}_{(k+1)\tau}]_m}{\sqrt{d}}\right)} \tag{59}$$

$$(\text{Triangle Inequality}) \leq \frac{\sum_{j=1}^{k\tau} \exp\left(\frac{[\mathbf{Q}_{k\tau}]_i^\top [\mathbf{K}_{k\tau}]_j}{\sqrt{d}}\right) \sum_{m=k\tau+1}^{(k+1)\tau} \exp\left(\frac{[\mathbf{Q}_{(k+1)\tau}]_i^\top [\mathbf{K}_{(k+1)\tau}]_m}{\sqrt{d}}\right) \cdot 2\|\mathbf{V}_m\|}{\sum_{j=1}^{k\tau} \exp\left(\frac{[\mathbf{Q}_{k\tau}]_i^\top [\mathbf{K}_{k\tau}]_j}{\sqrt{d}}\right) \cdot \sum_{m=1}^{(k+1)\tau} \exp\left(\frac{[\mathbf{Q}_{(k+1)\tau}]_i^\top [\mathbf{K}_{(k+1)\tau}]_m}{\sqrt{d}}\right)} \tag{60}$$

$$(\|\mathbf{V}_n\| \leq \epsilon, \ \forall n) \leq \frac{\sum_{m=k\tau+1}^{(k+1)\tau} \exp\left(\frac{[\mathbf{Q}_{(k+1)\tau}]_i^\top [\mathbf{K}_{(k+1)\tau}]_m}{\sqrt{d}}\right) \cdot 2\epsilon}{\sum_{m=1}^{(k+1)\tau} \exp\left(\frac{[\mathbf{Q}_{(k+1)\tau}]_i^\top [\mathbf{K}_{(k+1)\tau}]_m}{\sqrt{d}}\right)} \leq 2\epsilon \tag{61}$$

combined with the 960 hours of LibriSpeech-train. Model was trained using an initial learning rate of 1e-5, using an AdamW optimizer, weight decay of 0.01 for 2 epochs. We used a LoRA rank of 4, with points fraction $\hat{f} = 0.05$.